THE MECHANICAL PROPERTIES OF TANTALUM WITH SPECIAL REFERENCE TO THE DUCTILE-BRITTLE TRANSITION

TECHNICAL DOCUMENTARY REPORT NO. ASD TR 61-203
PART II

March 1963

Directorate of Materials and Processes
Aeronautical Systems Division
Air Force Systems Command
Wright-Patterson Air Force Base, Ohio

Project No. 7351, Task No. 735106

(Prepared under Contract AF 33(616)-7173 by Materials Research Corporation, Orangeburg, New York;
G. T. Murray, R. A. Burn, authors)

NOTICES

When Government drawings, specifications, or other data are used for any purpose other than in connection with a definitely related Government procurement operation, the United States Government thereby incurs no responsibility nor any obligation whatsoever; and the fact that the Government may have formulated, furnished, or in any way supplied the said drawings, specifications, or other data, is not to be regarded by implication or otherwise as in any manner licensing the holder or any other person or corporation, or conveying any rights or permission to manufacture, use, or sell any patented invention that may in any way be related thereto.

Qualified requesters may obtain copies of this report from the Armed Services Technical Information Agency, (ASTIA), Arlington Hall Station, Arlington 12, Virginia.

This report has been released to the Office of Technical Services, U.S. Department of Commerce, Washington 25, D.C., in stock quantities for sale to the general public.

Copies of this report should not be returned to the Aeronautical Systems Division unless return is required by security considerations, contractual obligations, or notice on a specific document.

26-623C, 500, 5-1-6

FOREWORD

This report was prepared by Materials Research Corporation under USAF Contract No. AF 33(616)-7173. This contract was initiated under Project No. 7351, "Metallic Materials", Task No. 735106, "Behavior of Metals". This work was administered under the direction of the Metals and Ceramics Laboratory, Directorate of Materials and Processes, Deputy for Technology, Aeronautical Systems Division with Mr. F. G. Ostermann acting as Project Engineer.

This report covers the work conducted from 1 April 1961 to 1 April 1962.

ACKNOWLEDGEMENTS

This work was suggested and initiated by Dr. M. A. Adams. The assistance of Mr. C. Malo and Mr. P. Salmaggi in material preparation is gratefully acknowledged.

ABSTRACT

The lower yield stress-grain size relationship was studied in tantalum for two compositions; one consisting of a total interstitial content of 72 ppm with the major constituent being oxygen, and the other containing primarily carbon (116 ppm) in which part of the carbon existed in the form of a finely dispersed carbide precipitate. These results were compared to those obtained earlier (1) on commercial tantalum containing a total interstitial content of about 200 ppm. The parameters σ_i and k_y in the Petch equation

$$\sigma_y = \sigma_i + k_y d^{-1/2}$$

were of primary interest. The commercial tantalum exhibited significantly higher yield and flow stresses and correspondingly higher σ_i values. The carbon containing material showed the lowest yield stresses primarily because of its lower oxygen content. It was concluded that oxygen is much more effective than carbon in restricting dislocation movement. The effect of the carbide precipitate was to increase the work-hardening rate. The flow stresses, however, even in the presence of the carbide phase were lower than those observed for commercial tantalum.

The k_y values obtained on the 72 ppm solute content materials for a strain rate of 10^{-1}/sec. were found to be approximately 2×10^7 c.g.s. units and thus about a factor of two larger than those found on commercial tantalum. For both materials k_y did not vary with test temperature at a strain rate of 10^{-3}/sec., however, at a strain rate of 10^{-1}/sec. k_y for the 72 ppm solute material was found to vary from about 1 to 3×10^7 c.g.s. with the larger values being measured at the lower test temperature. k_y values for the carbon containing material were found to be very small ($\sim 0.5 \times 10^7$ c.g.s.) and did not vary appreciably with test temperature or strain rate. It was suggested that this small k_y may be due to a large number of unlocked dislocations as a result of the carbide particles acting as sources.

k_y and σ_i values were also computed by the Lüders strain technique for the room temperature tests and found to agree reasonably well with those obtained by the grain size method.

This technical documentary report has been reviewed and is approved.

W. J. TRAPP
Chief, Strength and Dynamics Branch
Metals and Ceramics Laboratory
Directorate of Materials and Processes

TABLE OF CONTENTS

LIST OF ILLUSTRATIONS

LIST OF ILLUSTRATIONS
(Continued)

LIST OF TABLES

I. INTRODUCTION:

In an earlier study (1)* on specimens of commercial tantalum the variation of lower yield stress σ_y with grain size 2d was used to assess the effect of temperature and strain rate on the parameters σ_i and k_y in a Petch equation

$$\sigma_y = \sigma_i + k_y d^{-1/2} \qquad (1)$$

where σ_i represents the lattice friction stress and k_y is a measure of the dislocation locking strength. Cottrells' transition equation

$$(\sigma_i d^{1/2} + k_y) k_y = \beta \mu \gamma \qquad (2)$$

was used to compute an effective surface energy γ for crack propagation. Here μ is the shear modulus of the material and β a constant equal to unity for conventional tests, and 1/3 for tests on notched specimens. The theory (2)(3) underlying these two equations was critically reviewed in the earlier report and will not be repeated here.

In the earlier work (1) it was concluded that the sensitivity of the yield strength to temperature and strain rate arose almost entirely from the effects of these variables on σ_i. σ_i values were computed that varied from approximately 20.5 Kg/mm^2 at 298°K to 88 Kg/mm^2 at 77°K. A k_y value of 10^7 c.g.s. units was found that did not vary with temperature. From the observation of small cleavage facets on the fracture surfaces in the

* Numbers in parentheses indicate References

Manuscript released by the authors August 1962 for publication as an ASD Technical Documentary Report.

77°K test, γ was computed to be between 1.16 and 1.35 X 10^4 erg/cm^2. In an extension of this work (4) the fact that considerable deformation occurred in the necked region prior to fracture was taken into consideration. True stress-area reduction curves were then obtained and it was found that the flow stress prior to fracture was about a factor of two larger than the yield stress. Thus by increasing σ_i by a factor of two the new value of γ was then computed and was found to be between 2.3 and 2.7 X 10^4 erg/cm^2. It was thus concluded that tantalum derives its greater resistance to brittleness (compared to Nb, Mo, and steel) not only from its low value of k_y and high value of μ, but also from its high value of γ.

The present investigation was intended to extend the above study to tantalum containing controlled quantities of interstitial solute. It was decided to conduct the experiments as before at three temperatures and two strain rates but in addition to include the solute in two states - namely in solid solution and as a second phase. It was thought that the relative values of σ_i and k_y would be affected by the state of the solute distribution.

II. EXPERIMENTAL PROCEDURE:

Material in the form of 3/16" diameter rods of 99.9% pure tantalum was obtained from the Kawecki Chemical Corporation. These rods were given a double pass in a floating-zone electron beam zone refiner which was maintained at a minimum vacuum of 5 X 10^{-5} mm Hg. This zone refining equipment and operation has been described elsewhere (1)(5).

The total interstitial content in high vacuum beam melted material is dependent on the composition of the starting material and zoning speed. It has been demonstrated at Materials Research Corporation that the total content can be kept below 25 ppm by a suitable choice of these variables. However, this resulting high purity material often does not show a yield point, and when one is observed it is very small. Consequently, the starting material and zoning speeds were selected to give a somewhat larger interstitial content. This material, referred to hereafter as "high purity", yielded an average total interstitial content of 72 ppm with oxygen being the major constituent (see Table II).

In order to study the effect of carbide precipitate, rods of beam melted "high purity" material were coated with "Oil Dag" (a suspension of carbon in oil) by immersion and the oil subsequently burned off at 400°C to leave a surface layer of carbon. These "Dag-coated" rods were then remelted in the electron beam refiner which allowed the carbon to be homogeneously distributed

throughout the molten zone.

Both types of rods were then given a 77% reduction in area by cold rolling to 0.090" diameter and subsequently annealed in the electron beam at various power settings. The resulting grain sizes and annealing temperatures are listed in Table I. Temperatures were measured with an optical pyrometer. The actual value of grain size (2d) used in the Petch equation was determined by metallographic examination of each individual specimen after fracture. The average grain diameter was determined by counting the number of grains intersecting a diameter marker on a polished cross-section. The cross-section was taken in the gage section (outside the necked region) and corrections were made for grain size reduction as a result of the uniform reduction in area. It was found that specimens cut from the same recrystallized rod were essentially of the same grain size.

The "Dag-coated" specimens contained significant quantities of carbide precipitate after the recrystallization annealing treatments. Since these specimens were annealed at various temperatures, the carbide distribution as well as the amount of carbon in solid solution was expected to vary with the annealing temperature employed. The resulting homogeneous carbide distribution representative of several annealing temperatures is shown in Figure 1. The range of the annealing temperatures was about 400°C and it can be seen that the carbide distribution did not vary significantly over this range. It can be seen that, except for the smallest grain size specimens, considerable grain boundary carbide precipitate is present for certain boundary misorientations. These boundaries invariably possessed a narrow adjacent region which was totally void of visible precipitate. One would also expect the carbon in solution to vary with annealing temperature, however, an examination of the phase diagram (6) shows that over this temperature range the maximum change in solubility is only of the order of 20 ppm.

The chemical analyses for the interstitial content of the as-received, "high purity" and carbon doped materials are shown in Table II. For the latter two materials three specimens were selected at random for analysis and all three values are reported (National Research Corporation analyses; Kjeldahl technique used for nitrogen.) Note that the "Dag-coated" specimens contain less oxygen than the "high purity" rods from which they were processed. The added carbon assists in removal of oxygen. The as-received material contained significant quantities ($\sim$1000 ppm) of substitutional solute whereas in the beam melted material only about 40 ppm metallic solute was found. The analysis of the beam

recrystallized commercial material employed by Adams and Iannucci (1) is also included in TableII for comparison purposes.

Tensile test pieces were made by brazing the ends of 2" lengths of the recrystallized tantalum to threaded stainless steel collars as previously described (1). Brazing was carried out in the electron beam apparatus which produced a neat regular fillet leaving a 1" gage length. Each brazing operation took less than one minute, and metallographic examinations of numerous joints showed no grain growth in the tantalum as a result of the brazing. Tensile tests conducted on representative samples in the etched and un-etched condition showed no difference due to the surface removal. Consequently, the etching operation was discontinued.

The tensile tests were carried out in a "hard" machine of the type described by Adams (7) at temperatures of 298, 195 (acetone and dry-ice mixtures), and 77°K (liquid nitrogen). At each temperature specimens covering the range of grain sizes of $d^{-1/2}$ from 1.2 $mm^{-1/2}$ to 7.6 $mm^{-1/2}$ were tested at strain rates of 10^{-1} and 10^{-3}/sec. The stress-strain curves were autographically recorded on a milli-volt recorder whose rapid response time (1/4 sec. for full range deflection) resulted in high loading sensitivity.

III. RESULTS:

A. "High Purity" Material

1. General stress-strain behavior

The test conditions and resulting stress-strain and fracture data for each specimen tested are listed in Table III. Representative stress-strain curves for each temperature and strain rate are shown in Figure 2 for specimens of large grain size ($d^{-1/2} \sim 1.5$ $mm^{-1/2}$) and in Figure 3 for smaller ($d^{-1/2} \sim 5$ $mm^{-1/2}$) grain size specimens. The results were similar to the earlier work (1) in respect to comparative behavior. All specimens tested at 298 and 195°K (and most of those at 77°K) showed sharp well-defined yield points, and a low rate of strain hardening.

For a given grain size the upper and lower yield stresses increased and the elongation to fracture decreased with decreasing temperature. Increasing the strain rate increased the upper and lower yield stresses, as expected, and in most cases decreased the elongation to fracture. (The present 77°K behavior was somewhat different from that observed for commercial tantalum (1) in which the strain rate at 77°K had no effect on the lower yield stress.) The size of the yield drop did not appear to vary in

any well-defined fashion with either strain rate, temperature, or grain size. However, the "true" upper yield point is seldom realized in practice due to premature local yielding arising from random stress concentrations.

For a given strain rate and temperature the effect of an increase in grain size (decreasing $d^{-1/2}$) is to displace the curves to a lower stress level. Comparative stress-strain curves are shown in Figure 4. This comparison was similar for all grain sizes examined. Again, the 77°K behavior differed from that found in commercial tantalum (1) where reversal of behavior of lower yield stress with grain size was observed. In general, the elongation to fracture increased as the grain size decreased.

All specimens showed local necking and, once necking had commenced, continued to deform (to fracture) in the necked region. Area reductions in the necked region were greater than 90% and resulted in a ductile-type fracture. The majority of fractures were of the ragged shear type although a number of chisel edge types were found (see Table III for description of fracture surfaces). The preponderance of a given type did not appear to vary with test temperature or strain rate. A longitudinal section of a typical ductile fracture is shown in Figure 5. A microhardness traverse is also included to show the extent of work-hardening in the necked region. The results verify the conclusions of Adams and Iannucci (4) that the true flow stress in this region increases markedly. Some specimens showed small light reflecting facets (Figure 6) but these appeared in specimens tested at all temperatures. The facets did not correlate with the grain size implying that they are not grain boundary fractures. It should be pointed out that the facets do not appear to be as well developed as the cleavage facets found by Adams and Iannucci (1) in their 77°K tests.

2. The Petch relationship

The variation of lower yield stress with grain size was the main objective of the present investigation since this enables a determination of the σ_I and k_y parameters in the Petch equation. The lower yield stress-grain size data of Table III are plotted in Figure 7. For a given temperature and strain rate the data was fitted to a straight line using the method of least squares. Although the reproducibility for specimens of identical grain sizes and test conditions was excellent, there exists some departure of points from the computed straight line. This departure is larger at the 77°K test temperature.

However, the small increase in lower yield stress with decreasing grain size is believed to be a real effect.

The k_y and σ_i values determined from the straight lines of Figure 7 are listed in Table IV. Due to the slight variation of the lower yield stress with grain size the k_y values are estimated to be accurate within ± 50%. Within this accuracy k_y increases with decreasing test temperature for the low strain rate tests but shows little or no change with test temperature for the higher strain rate tests. The variation of k_y with strain rate was not as well defined showing an increase at room temperature and a decrease at the lower temperatures with increasing strain rate. The results for commercial tantalum yielded a similar value of k_y that did not vary with either test temperature or strain rate. The temperature variation of k_y for the "high purity" material is shown in Figure 8.

The values of σ_i (± 5% accuracy) increase with both decreasing test temperature and increasing strain rate. The σ_i variation with test temperature is shown in Figure 9.

B. Carbon Doped Material

1. General stress-strain behavior

The stress-strain and fracture data obtained on the carbon doped specimens are listed in Table V. Representative stress-strain curves for these specimens are shown in Figure 10 for large grain size specimens and in Figure 11 for smaller grain diameters. Again the usual behavior is noted, i.e., for a given grain size the yield and flow stresses increased with increasing strain rate and decreasing temperature, with corresponding reductions in elongation to fracture. Strain hardening in the low strain rate tests at 298 and 195°K was somewhat larger than that found in "high purity" or commercial tantalum. Of particular significance here is the unusually large elongation to fracture obtained at 77°K (particularly at small grain sizes) and the fact that this elongation was larger for the higher strain rate tests. As a result the yield drops were particularly well defined in contrast with the yield drops on commercial and "high purity" tantalum at 77°K. The size of the yield drops did not follow any particular pattern with respect to temperature, strain rate or grain size.

For a fixed strain rate and temperature the curves were generally displaced to lower flow stress levels for larger grain size specimens although the yield stresses did not differ significantly. Small grain size specimens tested at 77°K were exceptions to this generalization. In general the elongation to

fracture increased with decreasing grain size. At 77°K this elongation was surprisingly large and not only increased with decreasing grain size but was larger at the higher strain rate.

The carbon doped specimens also showed typical ductile-type fractures with 90% or larger reduction in area in the necked region. In fact this necking was more pronounced than for the "high purity" specimens. A longitudinal cross-section of the necked region is shown in Figure 12. The included microhardness traverse demonstrates the extent of strain hardening in the deformed region. The larger strain hardening in this case as compared with the "high purity" material (Figure 5) can be attributed to both the greater deformation (grain sizes are similar) and higher carbon content of the carbon doped material. This point will be further discussed in terms of strain hardening coefficients.

In all of the large grain size carbon doped samples it was clear from photographs such as Figure 12 that fracture did not occur at the grain boundaries as one might expect in view of the grain boundary precipitate. In the smaller grain size specimens the presence or absence of grain boundary fracture could not be ascertained by microscopic examination of the longitudinal cross-sections.

Microscopic examination of the fracture surfaces revealed light-reflecting facets on only a relatively few specimens and these were extremely ill-defined. It is believed that neither cleavage nor grain boundary fracture occurred in the carbon doped samples.

2. The Petch relationship

The lower yield stress-grain size plot is shown in Figure 13 for each of the six test conditions. The straight lines were again computed by the method of least squares. Fewer carbon doped specimens were tested than for the "high purity" case but the range of grain sizes tested was larger than in the "high purity" material where small grain sizes were difficult to obtain. Evidently the interstitial carbon in solution restricts grain growth upon recrystallization. The k_y and σ_i values determined from these plots are listed in Table VI. The negative slope obtained at the low rate test at 195°K is not significant within the stated experimental accuracy. It is believed that k_y does not vary with temperature at 298 and 195°K in carbon doped "high purity" tantalum. Furthermore the values appear to be extremely small, i.e., the grain size dependence of the lower yield stress in

the carbon doped material is nil.

The behavior at 77°K is difficult to explain. At the low strain rate a small positive value of k_y is obtained but at the high strain rate a sizable negative value is computed. Adams and Iannucci (1) also noted a peculiar behavior at 77°K for commercial tantalum in that below a certain grain size the yield stress decreased. It was suggested that this decrease might be due to the inability of the grain boundaries to arrest the dislocations from the initial strong yielding pulse. In the present work the data at the low strain rate were not obtained at sufficiently small grain sizes to ascertain whether or not a decrease in yield stress existed at these grain sizes (these tests are planned). The high strain rate tests did show a yield stress decrease at small grain sizes and could possibly be associated with the mechanism described by Adams, et al.

The σ_i values are plotted as a function of test temperature in Figure 14. They vary with temperature and strain rate in the expected fashion.

C. Comparative Behavior of "High Purity", Carbon Doped, and Commercial Tantalum

It is of interest now to compare the behavior of the three tantalum compositions, the commercial tantalum results being taken from the work of Adams and Iannucci (1).

Comparative stress-elongation curves for similar grain sizes at temperatures of 77 and 298°K and at a strain rate of 10^{-1}/sec. are shown in Figure 15. The most readily observable differences are the significantly higher yield stresses at all test temperatures and the higher flow stresses at room temperature of the commercial material as compared with the "high purity" and carbon doped materials. This can be attributed to the higher interstitial content, noticeably oxygen, of the commercial material.

In comparing the "high purity" and carbon doped curves it can be seen that the carbon doped specimens showed slightly lower yield stresses but a greater rate of work-hardening than the "high purity" samples. This same behavior was observed at other temperatures, grain sizes, and strain rates. The lower yield stress of carbon doped samples is in part related to their lower oxygen content, and, as discussed later, the carbide particles acting as dislocation sources may also be important.

These tests illustrate that interstitial oxygen is much more effective than carbon for restricting dislocation movement. Whether

locking or lattice friction stress is more important will be discussed later. All oxygen is in solution and based on reported solubility (6) for carbon in tantalum, it is estimated that about 100 ppm carbon is retained in solution in the carbon doped material after the recrystallization anneal.

The carbon doped samples also exhibit more strain hardening than the other materials. The strain hardening coefficients of the room temperature curves shown in Figure 15 were obtained from the relationship

$$\sigma = K\epsilon^{n}$$

where σ = true stress

ϵ = true strain

K = constant

and n = strain hardening coefficient

These values are listed in Table VII. The fine carbide particle distribution gives rise to dispersion hardening and hence a larger value of n.

The 77°K tests show another significant difference between the carbon doped and other samples. The carbon doped specimen exhibits a much larger uniform elongation prior to necking. This larger elongation is directly related to the dispersion hardening created by the presence of the carbide particles, i.e., an increased restriction of necking brought on by the increased strain hardening. This ductility in the carbon doped specimens at 77°K was not so pronounced at large grain sizes and low strain rates, but was measurably larger than for the other two compositions. The large grain size and low strain rate tests also showed a less pronounced difference in yield stresses for the three compositions, a factor which would tend to minimize the relative difference in the onset of necking.

Comparative lower yield stress-grain size plots for 298 and 195°K at a strain rate of 10^{-1}/sec. for the three materials are shown in Figure 16. One can see that at all grain sizes the lower yield stresses of the commercial tantalum are considerably higher than for the other two materials with the "high purity"

material being slightly higher than the carbon doped material for all grain sizes tested. Note, however, that the extrapolated $\bar{\sigma}_i$ value for the carbon doped material is larger than that for the "high purity." The variation of $\bar{\sigma}_i$ with temperature is compared in Figures 17 and 18.

k_y varied significantly with temperature only in the "high purity" material, the range of values being from 0.65 to 3.4 X 10^7 c.g.s. units compared to a constant value of 10^7 for the commercial material and a low ($\sim$0.3 X 10^7) value for the carbon doped material.

D. Comparison with the Results of Other Investigations

Two studies similar to the present one have been recently reported. Owen, et al. (8) studied the effects of the interstitials, carbon, oxygen, and nitrogen in tantalum on the grain size-yield stress relationship and Koo (9) performed a similar study using a "high purity" vacuum melted tantalum with a total interstitial content of 25 to 82 ppm with carbon being the major constituent. These results are compared to those of the present study in Figure 19. It must be realized that the strain rates used by Owen, et al. and Koo were respectively 16 and 5 times smaller than the present strain rate of 10^{-3}/sec. Thus their curves are displaced slightly lower than they would be if the 10^{-3}/sec. strain rate of the present work had been used.

With respect to the strength levels it is again readily apparent that oxygen is of prime importance since the 147 ppm O_2 of Owen et al. shows higher yield strengths than does the 82 ppm O_2 commercial material, which in turn shows higher strengths than do the 40 ppm O_2 "high purity" and the 3 to 20 ppm O_2 materials (Koo). With respect to the grain size dependence of the yield strength, i.e., the k_y values, the larger oxygen content materials show the larger slopes with the one exception, that of the work of Koo. The authors "high purity" plot here seems of unusually small slope compared to the faster strain rate tests (Figures 7 and 16) and the results of Koo. At other test temperatures the present "high purity" results agree with those of Koo. More tests at smaller grain sizes are needed for increased accuracy. These tests are planned. The carbon containing material of Owen et al. yielded a small k_y value as did the present carbon doped material. However, their material presumably consisted of one phase and, as will be pointed out later, the low k_y is probably due to the low total solute content. It is somewhat surprising that this material showed yield strengths above the writers "high purity" material. The original data of Owen et al. showed considerable scatter and it may be that further experimental

investigation of this point is necessary.

The values of k_y computed by Owen et al. from their yield stress-grain size data varied from about 0.5 to 2.5 X 10^7 c.g.s. These authors computed much larger values of k_y (up to 10^8) by the Luders strain method and these values varied with test temperature and grain size (recrystallization temperature) the k_y values being smaller for small grain size specimens. As a check on the present work k_y and σ_i values were computed by the Lüders strain method (using log true stress/log true strain extrapolation) for the extreme grain sizes in "high purity" specimens tested at room temperature. The values are compared to the corresponding yield stress-grain size plot values in Table VIII. The present Lüders strain k_y also varies with grain size, being smaller for the smaller grain size specimens but does not differ greatly from the yield stress-grain size plot values. In the author's opinion the Lüders strain method is not accurate. This criticism has been voiced by others (3)(10).

IV. DISCUSSION

The Petch equation was derived on the premise that dislocations are locked by impurity atmospheres, and that the Lüders band propagates via dislocation pile-up at grain boundaries in yielded grains until their stress fields plus the applied stress activate sources in adjacent grains. To release these sources a stress σ_D is required which is

$$\sigma_D = (\sigma_y - \sigma_i)(d/\ell)^{1/2} \qquad (3)$$

where ℓ is the distance to the source from the pile-up at the grain boundary. Setting

$$k_y = \sigma_D \ell^{1/2} \qquad (4)$$

and rearranging, results in equation (1), i.e., the Petch equation. Thus the locking parameter k_y is also a function of source spacing. σ_i, the lattice friction stress, is usually regarded as being composed of two terms, σ_i^1 a temperature independent term arising from impurities and imperfections, and σ_i^{11} a temperature dependent term attributable to the Peierls-Nabarro stress of the lattice.

These concepts have recently been criticized rather extensively. Johnson (11) modified the original theory such that it would better agree with more recent experimental results by postulating that it is more difficult to propagate a Lüders band through a polycrystal than a single crystal because the regions near the grain boundaries

in a polycrystal are severely work-hardened. A more extensive criticism of the Petch relationship has been presented by Hahn (12). He developed an alternate approach, valid for both single crystals and polycrystalline bcc metals, based on a concept presented by Wilman and Johnston (13) to account for their observed yield drop in LiF. Essentially this approach is based on the assumption that locked dislocations remain locked and that the yield drop is a result of unlocked dislocations that multiply rapidly at a velocity which is stress dependent. Hahn accounted for the yield drop, continuous yielding, and delay time, however, the theory was not extended to include the grain size dependence of the yield stress.

The concept of yielding via unlocked sources can be used in conjunction with the original Petch equation to explain some of the present observations. The pertinent observations are as follows:

(a) k_y for carbon doped two phase material is extremely low, i.e., the yield stress is essentially independent of grain size.
(b) σ_i (commercial material) $> \sigma_i$ (carbon doped) $\approx \sigma_i$ ("high purity").
(c) For a given grain size and test condition , the magnitude of the yield stress decreases in going from commercial to "high purity" to carbon doped material.
(d) For a given grain size and test condition the flow stress is in the order of commercial > carbon doped > "high purity".
(e) The work-hardening coefficient of carbon doped tantalum is larger than that of the "high purity".
(f) The elongation to fracture at low temperatures is significantly larger in the carbon doped than in the other materials.

Following the unlocked source approach, the locking parameter k_y should be dependent on the number of unlocked sources, and the stress to cause these to propagate at a velocity sufficient for multiplication. The low k_y values in the carbon doped specimens can be explained in terms of the finely distributed carbide particles which act as dislocation sources. Due to thermal stresses unpinned dislocations can be generated at temperatures below that required for strain aging. This phenomenon has been demonstrated by Stokes (14). Thus a finely distributed second phase should increase the number of mobile dislocations available for motion and result in less locking and a smaller grain size dependence of the yield stress, i.e., both σ_D and ℓ are smaller where now σ_D represents the stress required to activate unlocked sources in adjacent grains. The lower oxygen content of the carbon doped material would likewise favor less locking of dislocations by means of elastic interaction.

Further support for the effect of a finely dispersed second phase in

yielding behavior can be obtained from an examination of the size of the yield drop. According to the Johnston and Gilman theory, an increase in the number of initially mobile dislocations considerably reduces the yield stress and the magnitude of the yield drop. Although the magnitude of the yield drop exhibited much scatter and did not vary in any well-defined pattern with grain size, strain rate, or temperature, an average of all tests showed that the magnitude of the yield drop in the carbon doped material was smaller by a factor of 2 than in the "high purity" and significantly smaller, by a factor of 4, than in the commercial tantalum. Furthermore the measured yield stress in the carbon doped material was smaller than for the other two materials.

The comparative values of the yield stress for the commercial and "high purity" single phase materials can be explained almost entirely on the basis of the impurity content. The larger interstitial content (particularly oxygen) of the commercial material reduces the number of initially mobile dislocations thereby raising the upper yield stress. Although the size of the yield drop is larger in the commercial material the lower yield stress and flow stress remains significantly above that observed for the "high purity" material. This higher stress level in the impure material accounts for the larger σ_i values obtained from the grain size plots and thus reflects a larger lattice friction stress according to the Petch theory. Hahn (12) derived an equation of state in which the stress level is largely dependent on a parameter related to the stress required for unit dislocation velocity. The physical significance of this parameter and σ_i are probably the same and in this respect the two theories do not differ.

Except for the low strain rate/room temperature tests, k_y for the "high purity" tantalum was larger by a factor of 2 to 3 than for the commercial material. This result is difficult to explain with either theory. One would expect a smaller number of mobile dislocations in the commercial material and as a result a larger k_y. The measurements of Koo (9) on a material of higher purity than the commercial material also showed higher k_y values which, except for the low strain rate/room temperature tests, are in good agreement with the present results. Owen et al. also obtained higher k_y values on their oxygen containing material, but there the oxygen content was larger than that of the commercial material and a higher k_y would be expected. These differences cannot be resolved at present. It must be realized that k_y cannot be measured accurately when the grain size effect is small and furthermore, that changes in chemistry and structure with recrystallization temperature certainly will affect the experimentally determined k_y. Also, the theories are not sufficiently developed at present to account for all experimental observations.

The larger work-hardening coefficient and larger elongation to fracture of the carbon doped material can be accounted for on the basis of the dispersion hardening caused by the carbide precipitate particles. The larger amount of elongation is directly related to increased restriction to necking as a result of the increased work-hardening.

V. BIBLIOGRAPHY

1. Adams, M.A., and Iannucci, A., ASD Technical Report 61-203, Contract No. AF 33(616)-7173 (1961).

2. Petch, N.J., Phil. Mag. 3, 1089 (1958).

3. Cottrell, A.H., Trans. AIME 212, 192 (1958).

4. Adams, M.A., and Iannucci, A., Materials Research Corporation Report No. 250, 4th Quarterly Progress, Contract AF 33(616)-7173 (August, 1961).

5. Adams, M.A., and Malo, C., Metals Progress, to be published.

6. D.M.I.C., Battelle Memorial Inst., Report No. 152, Contract AF 33(616)-7747 (April, 1961).

7. Adams, M.A., J. Sci. Instruments, 36, 444 (1959).

8. Owen, W.S. et al., Manufacturing Laboratories, Progress Report No. 3, Contract AF 33(616)-6838 (November, 1961).

9. Koo, R.C., J. Less Common Metals, 4, 138 (April, 1962).

10. Meakin, J.D., Acta Met., 9, 521 (1961).

11. Johnson, A.A., Phil. Mag., 7, 177 (1962).

12. Hahn, G.T., Acta Met., 10, 727 (August, 1962).

13. Johnston, W.G., and Gilman, J.J., J. App. Phys., 30, 129 (1959).

14. Stokes, R.J., submitted to Trans. AIME.

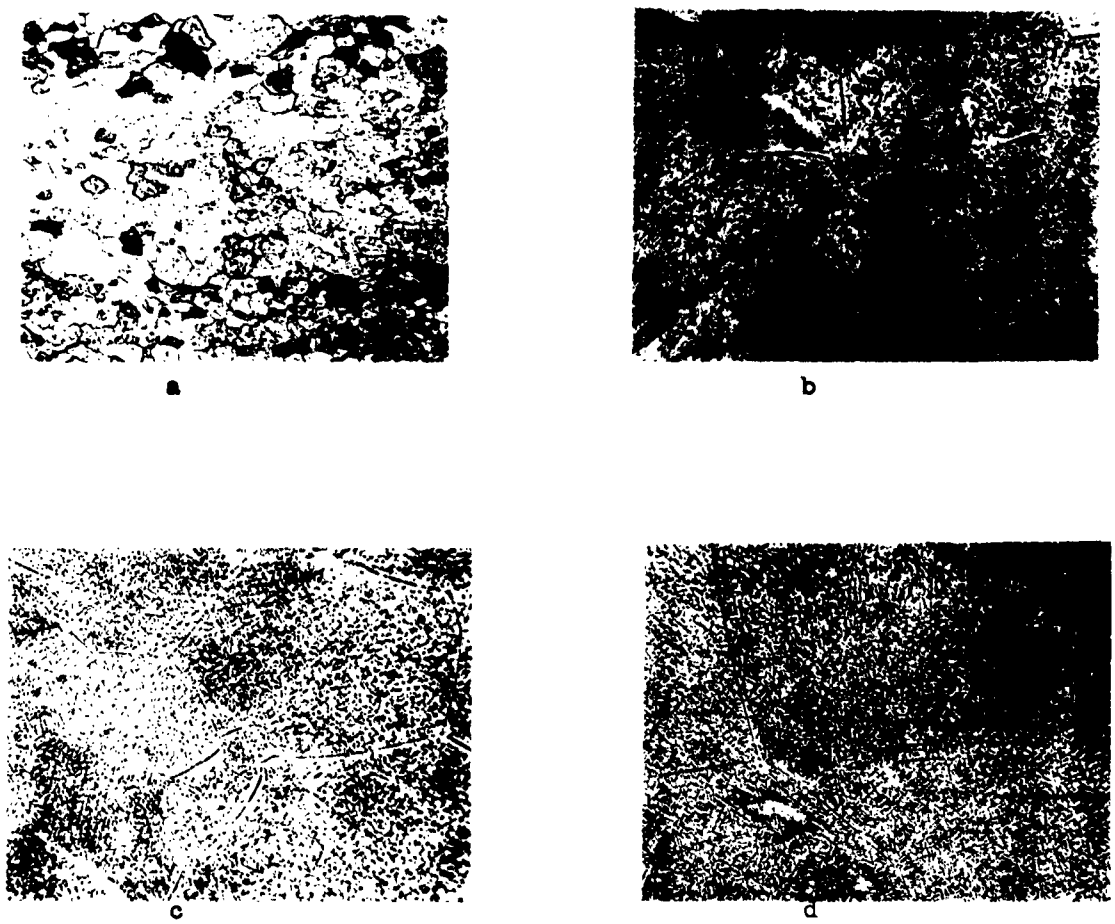

FIG. 1

Microstructures of carbon doped material recrystallized at (a) 1300°C; (b) 1440°C; (c) 1510°C; (d) 1720°C. Mag. X100.

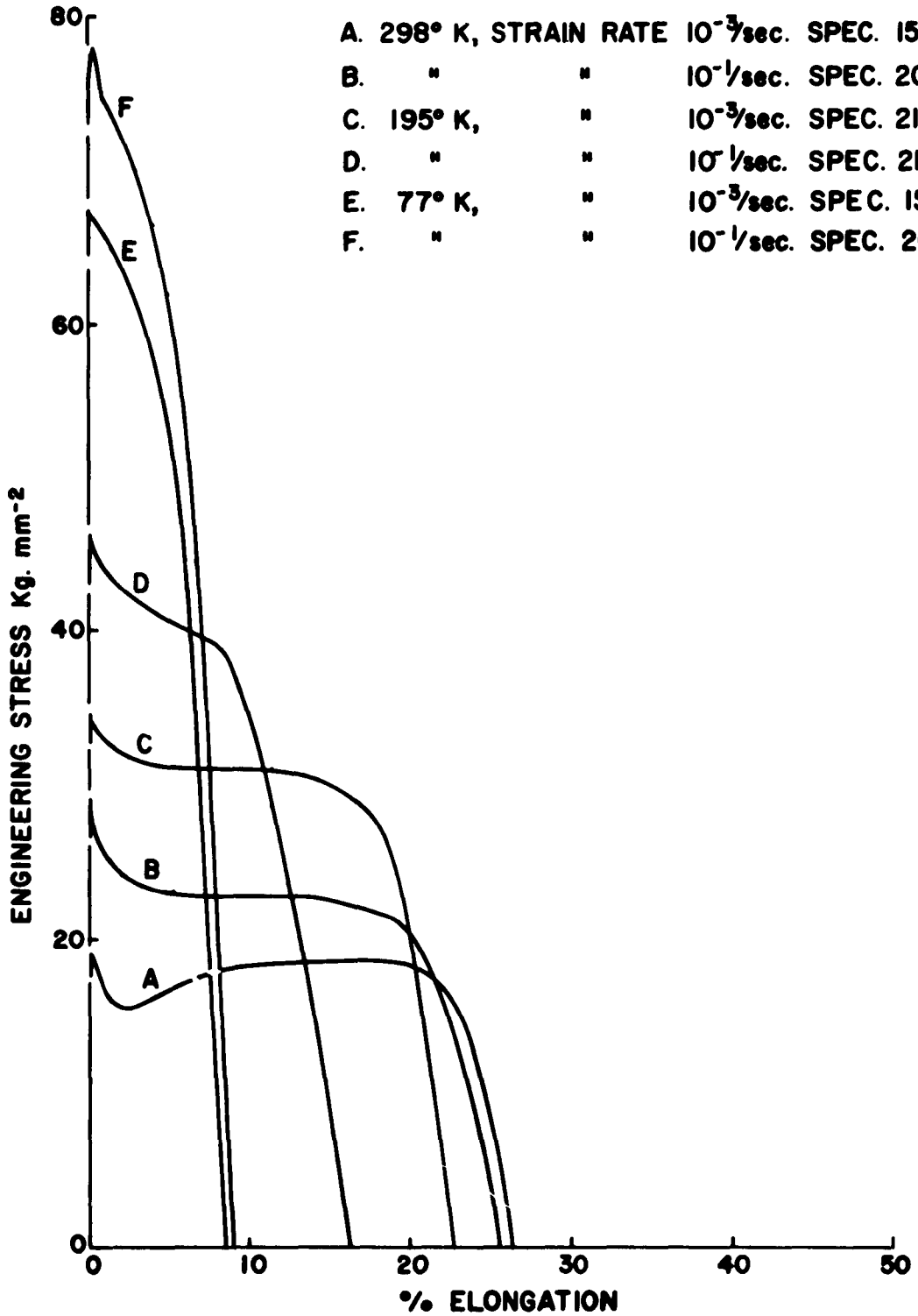

FIG. 2. REPRESENTATIVE STRESS-ELONGATION CURVES FOR "HIGH PURITY" SPECIMENS WITH $d^{-1/2}$ VALUES IN THE RANGE 1.25 TO 2.0 $mm^{-1/2}$

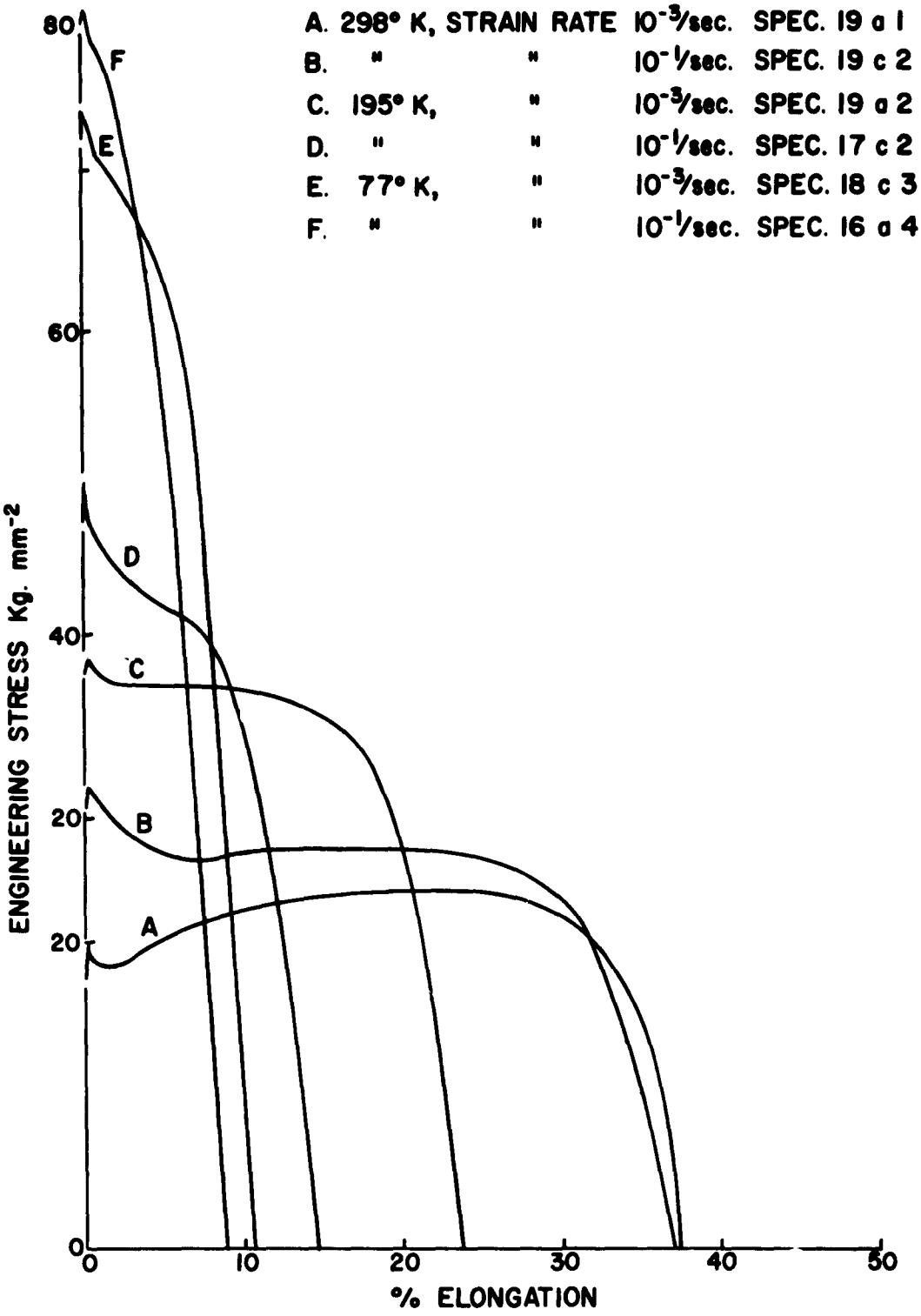

FIG. 3. REPRESENTATIVE STRESS-ELONGATION CURVES FOR "HIGH PURITY" SPECIMENS WITH $d^{-1/2}$ VALUES IN THE RANGE 4.4 TO 5.5 $mm^{-1/2}$

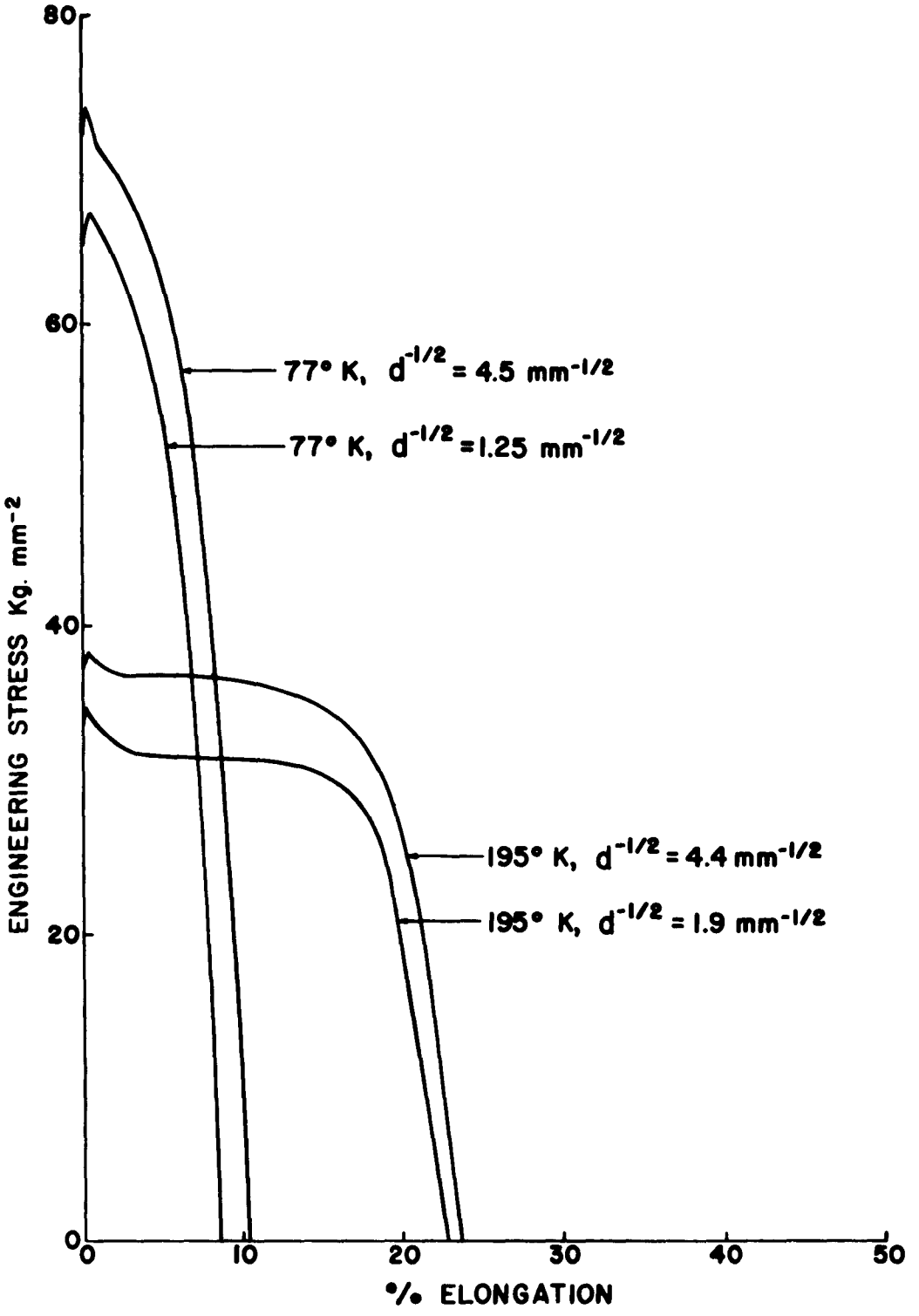

FIG. 4 EFFECT OF GRAIN SIZE ON STRESS-ELONGATION CURVES OF "HIGH PURITY" SPECIMENS AT A STRAIN RATE OF 10^{-3}/sec

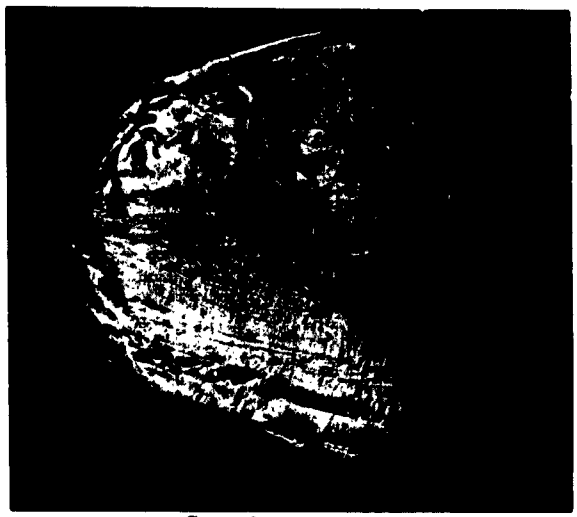

Specimen B17Q3
Test temp. 77°K-strain rate 10^{-3}/sec.

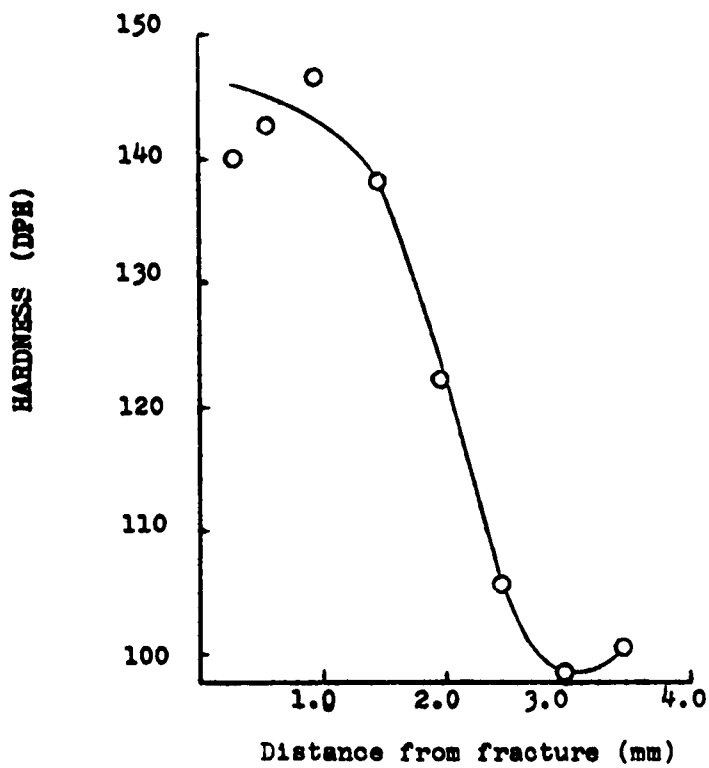

Fig 5. Longitudinal section of fracture zone. Hardness traverse shows extent of strain hardening in necked region. Spec. B17c3. Mag. X50.

FIG. 6

Light reflecting facet on fracture surface of specimen 20c1. Mag. X400.

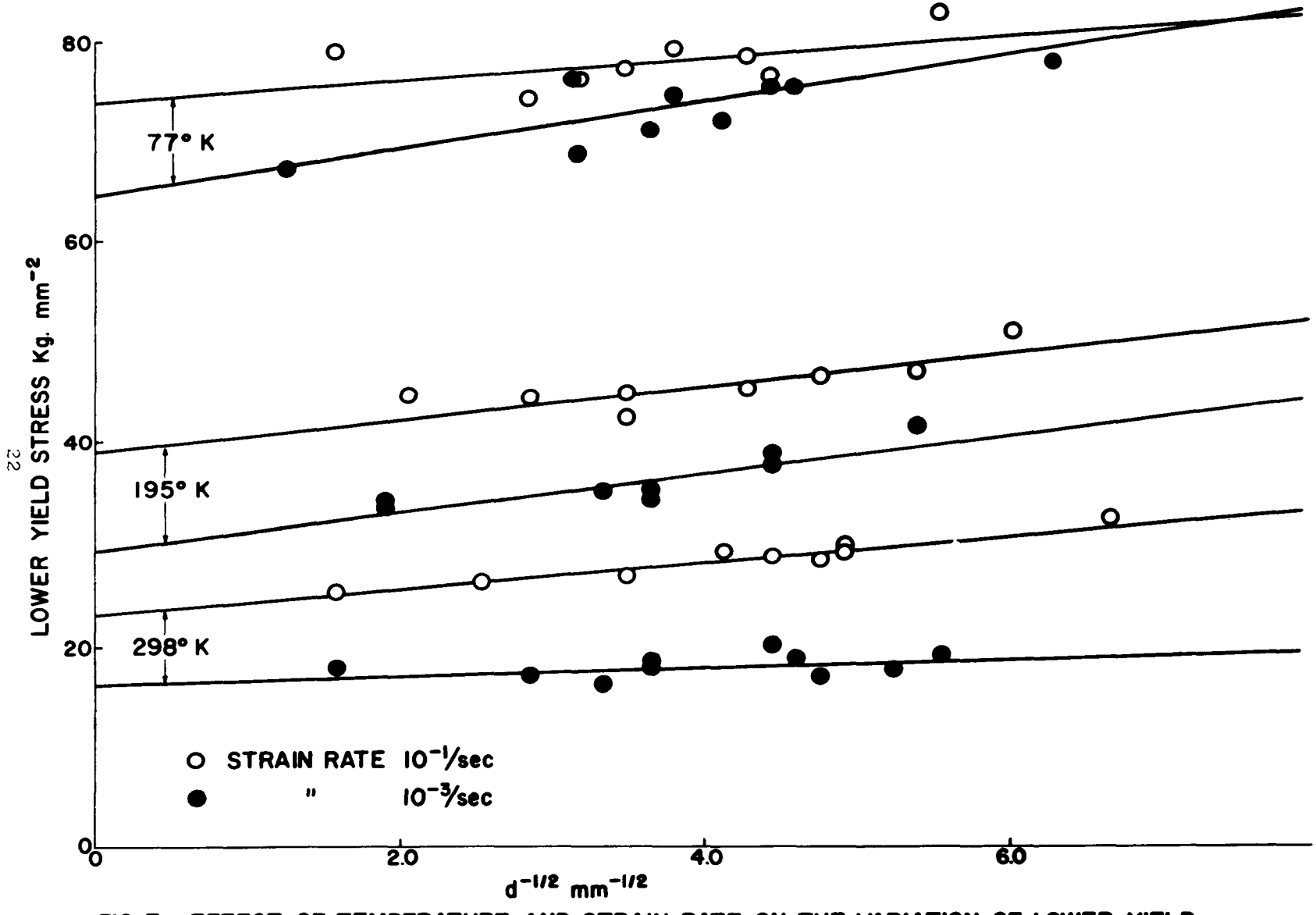

FIG. 7. EFFECT OF TEMPERATURE AND STRAIN RATE ON THE VARIATION OF LOWER YIELD STRESS WITH GRAIN SIZE FOR "HIGH PURITY" MATERIAL.

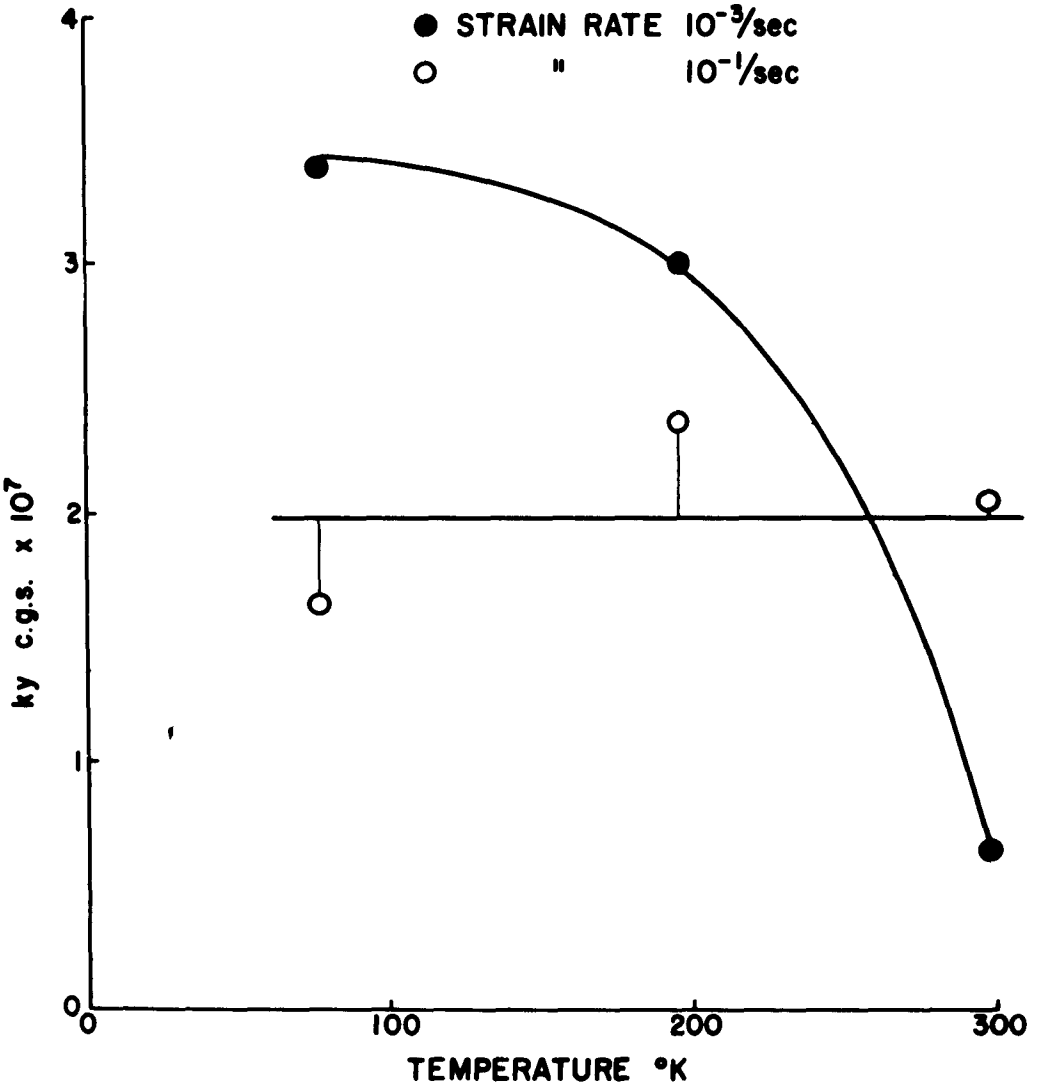

FIG. 8. THE VARIATION OF k_y WITH TEST TEMPERATURE FOR "HIGH PURITY" MATERIAL.

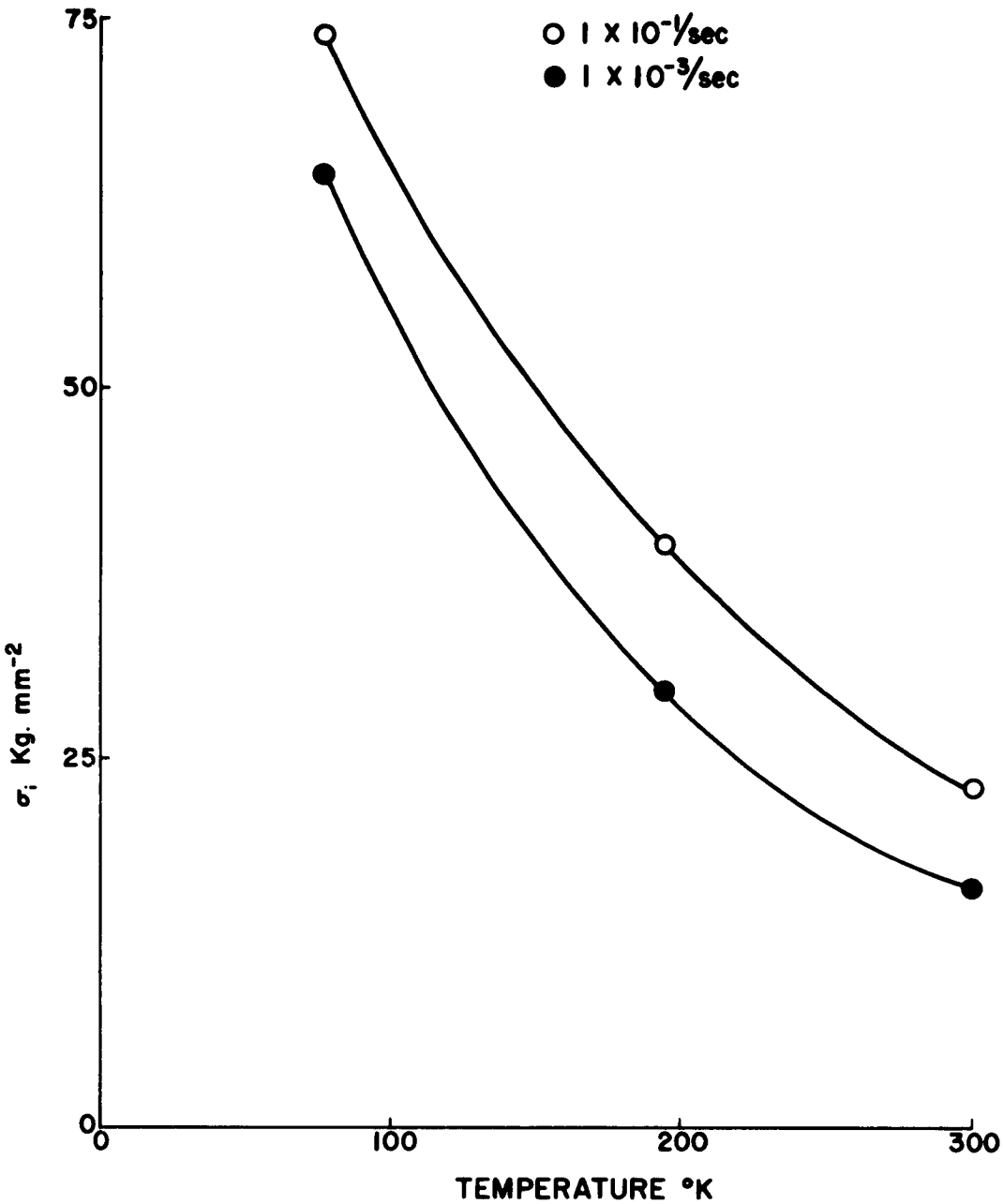

FIG. 9. THE VARIATION OF σ_i WITH TEST TEMPERATURE FOR "HIGH PURITY" MATERIAL.

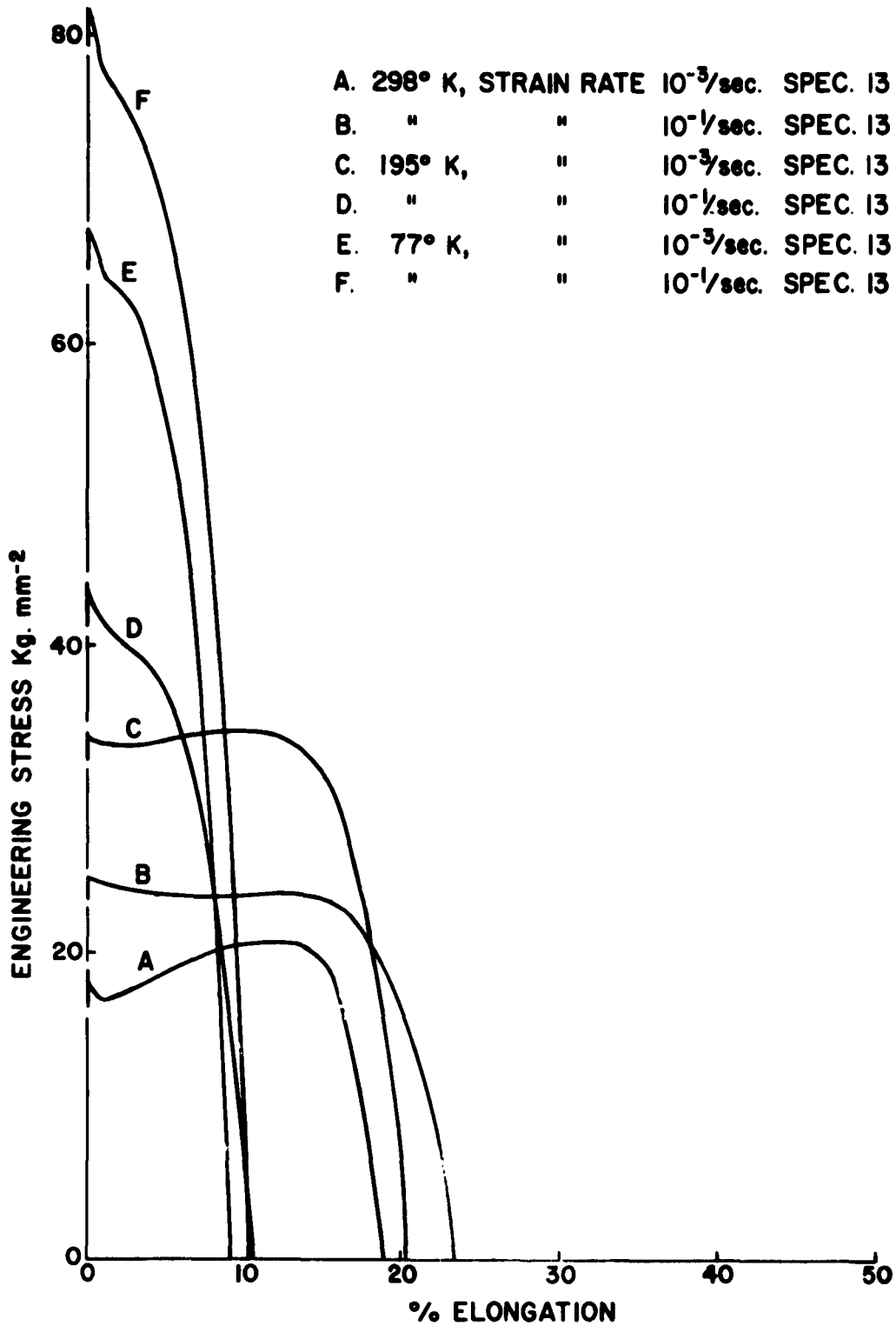

FIG. 10. REPRESENTATIVE STRESS-ELONGATION CURVES FOR CARBON DOPED MATERIAL WITH $d^{-1/2}$ VALUES IN THE RANGE 1.5 TO 2.2 $mm^{-1/2}$

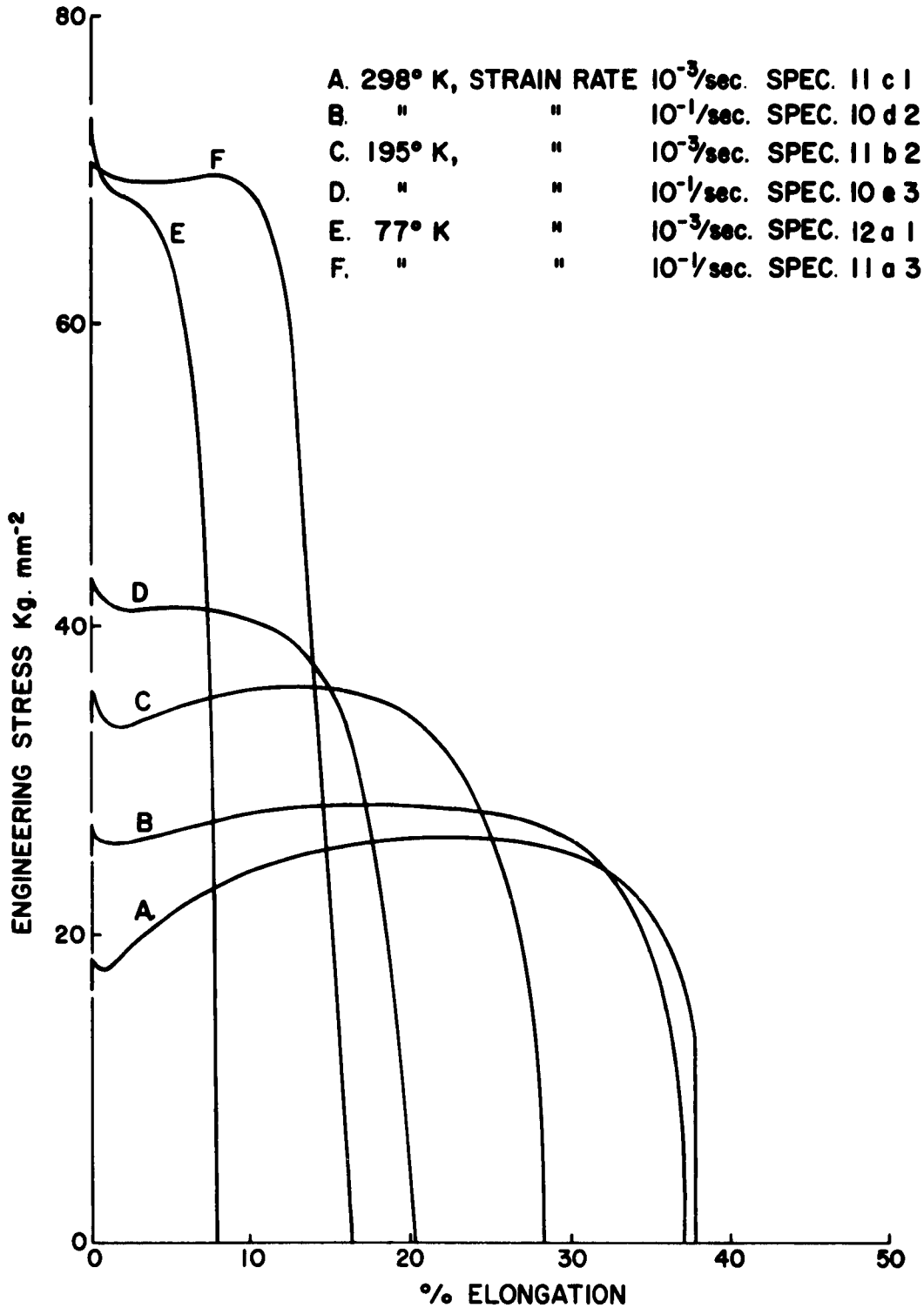

FIG. 11. REPRESENTATIVE STRESS-ELONGATION CURVES FOR CARBON DOPED MATERIAL WITH $d^{-1/2}$ VALUES IN THE RANGE 4.5 TO 5.6 mm.$^{-1/2}$

Specimen B22a
Test temp. 77°K-strain rate 10^{-3}/sec.

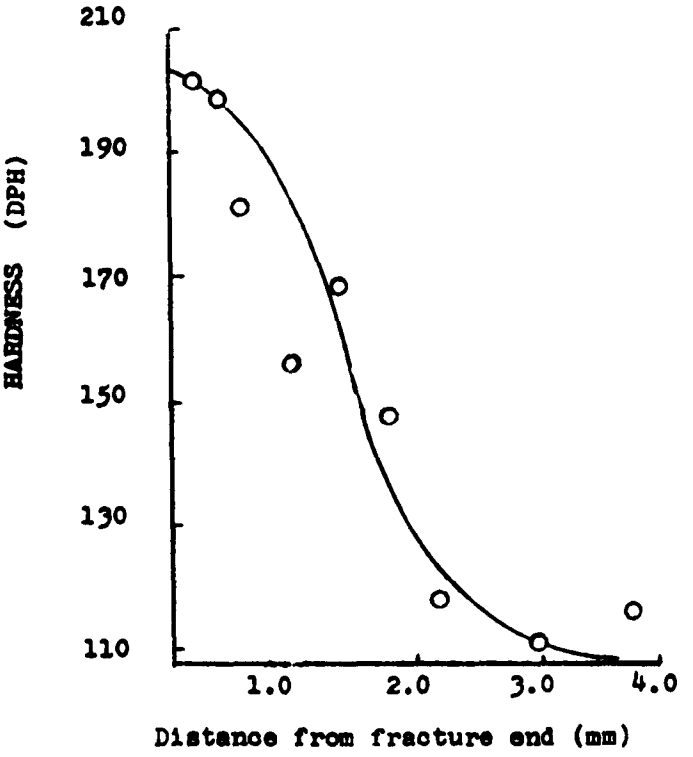

Fig 12. Longitudinal section through fracture zone of carbon doped specimen B22A. Mag. X50. Hardness traverse shows extent of strain hardening in necked zone.

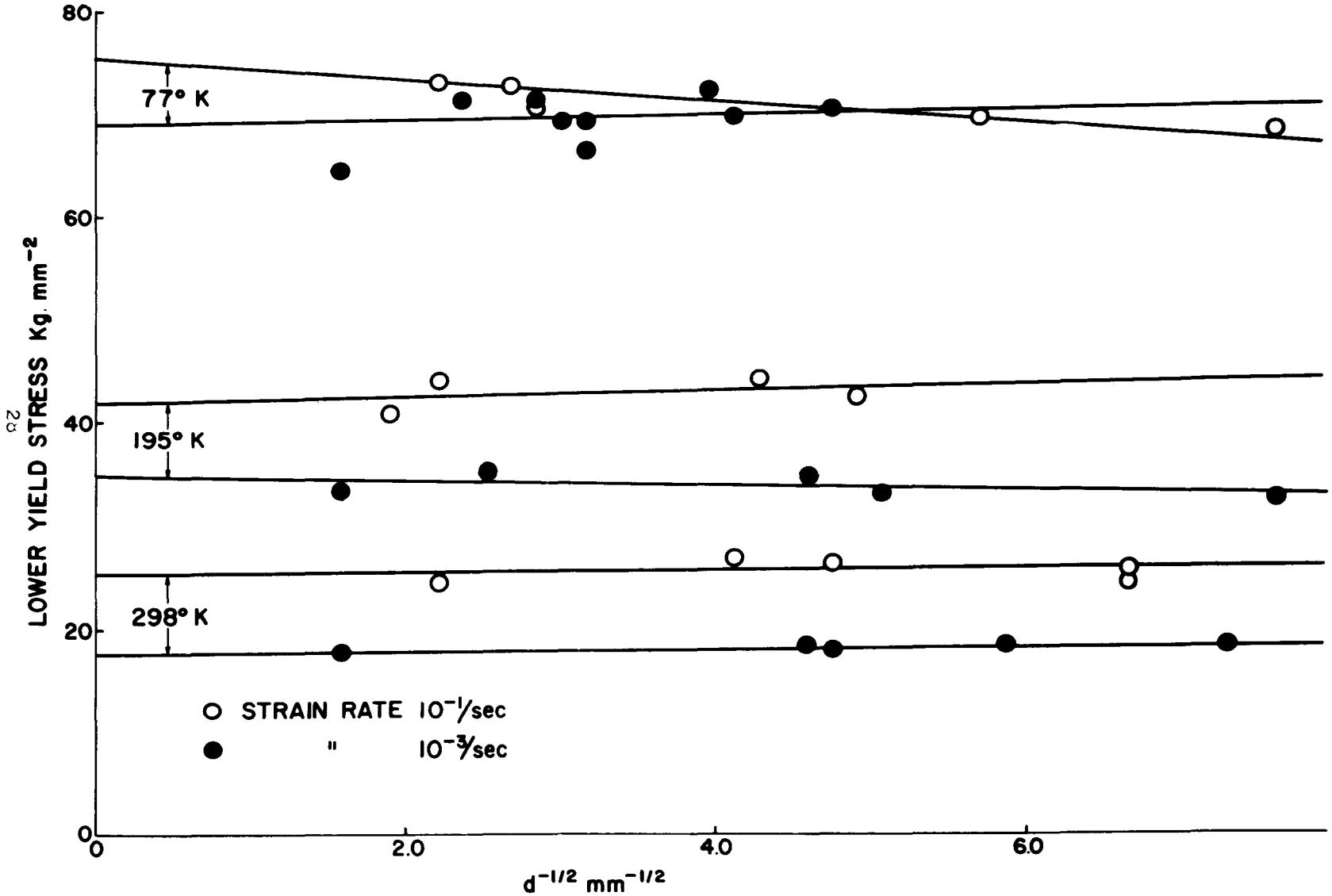

FIG. 13. EFFECT OF TEMPERATURE AND STRAIN RATE ON THE VARIATION OF LOWER YIELD STRESS WITH GRAIN SIZE FOR CARBON DOPED MATERIAL.

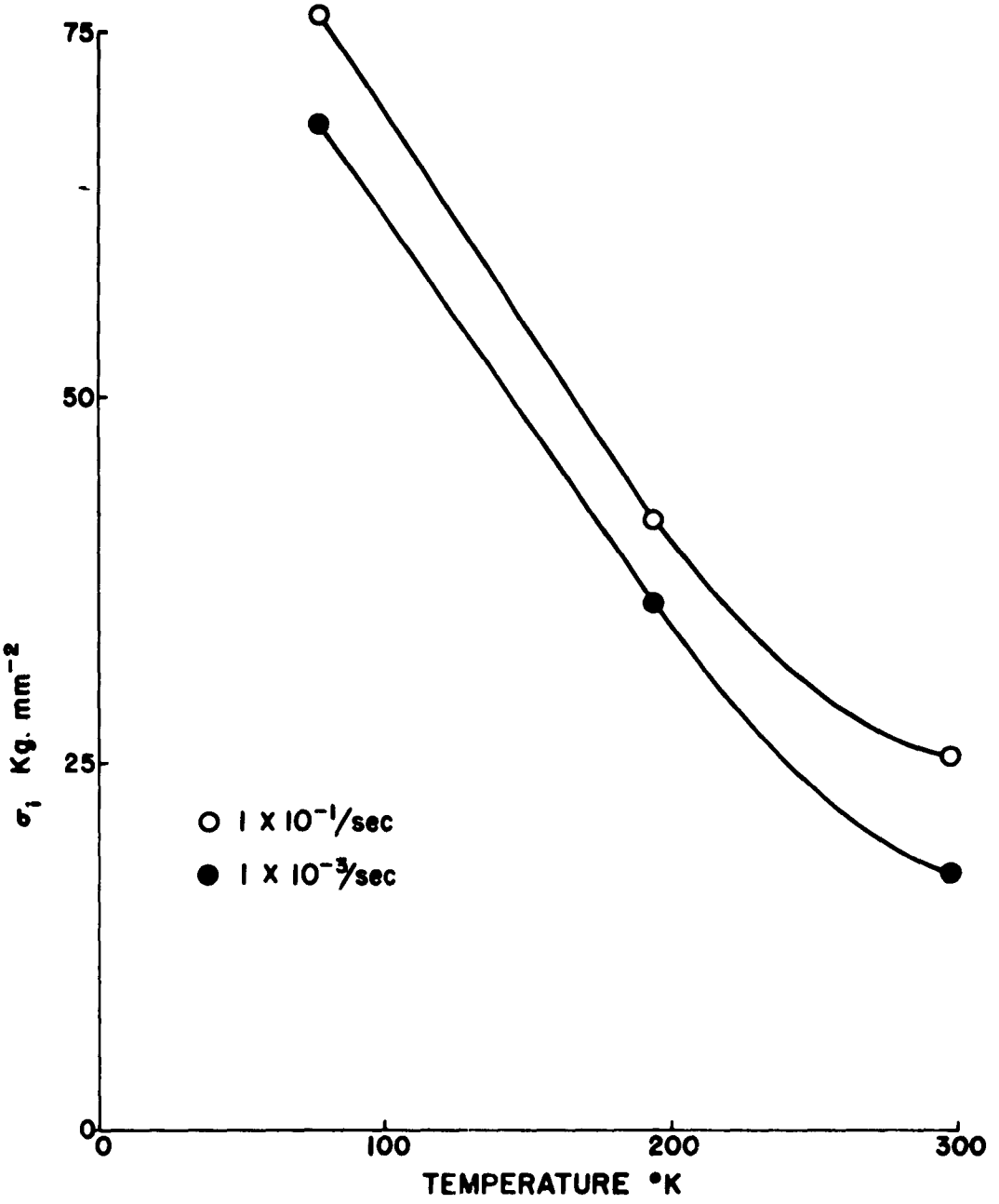

FIG. 14. THE VARIATION OF σ_i WITH TEST TEMPERATURE FOR CARBON DOPED MATERIAL.

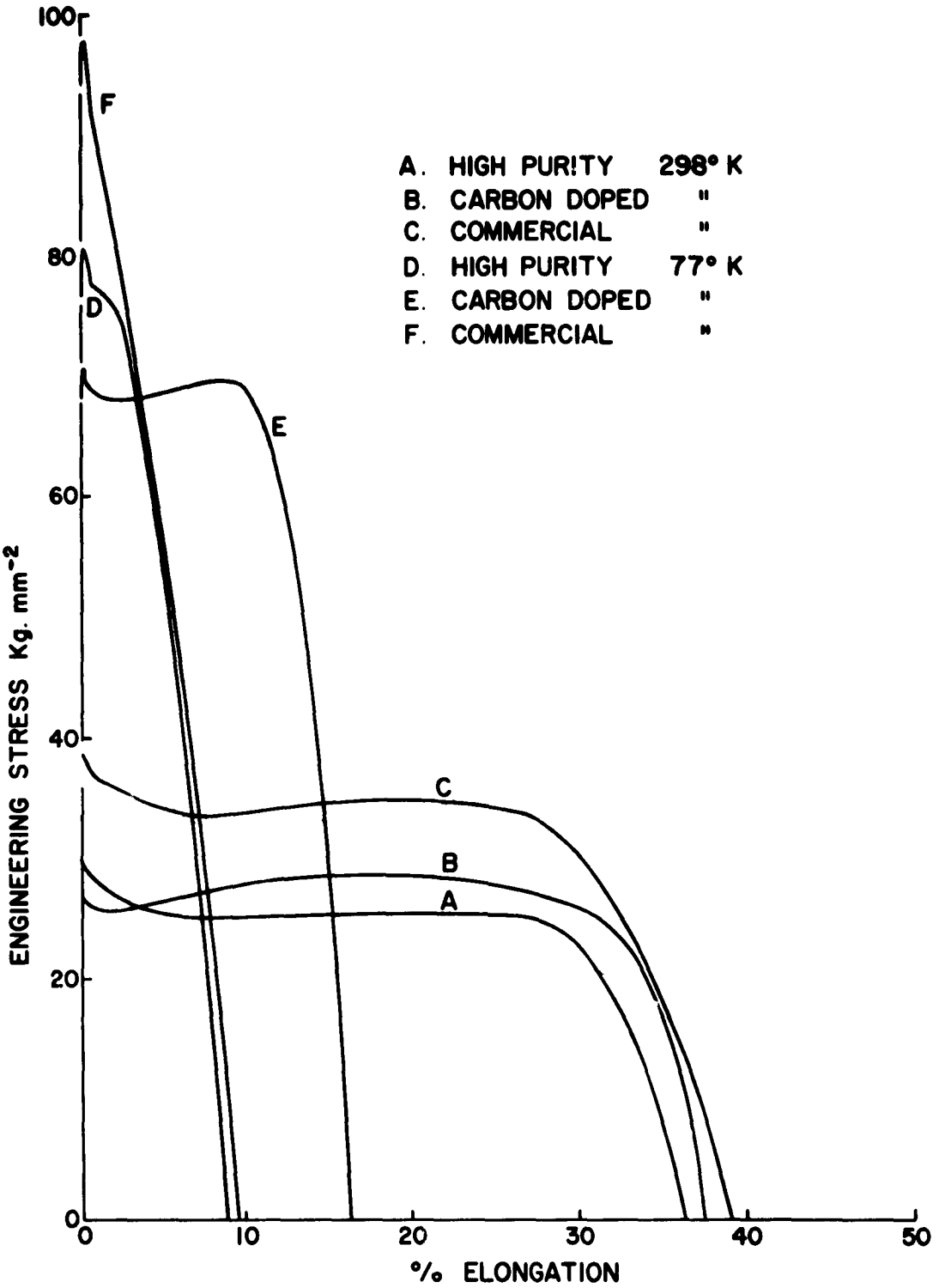

FIG. 15. COMPARATIVE STRESS-ELONGATION CURVES AT 298 AND 77° K AND AT A STRAIN RATE OF 10^{-1}/sec FOR $d^{-1/2}$ VALUES IN THE RANGE 4.5 TO 5.6 $mm^{-1/2}$

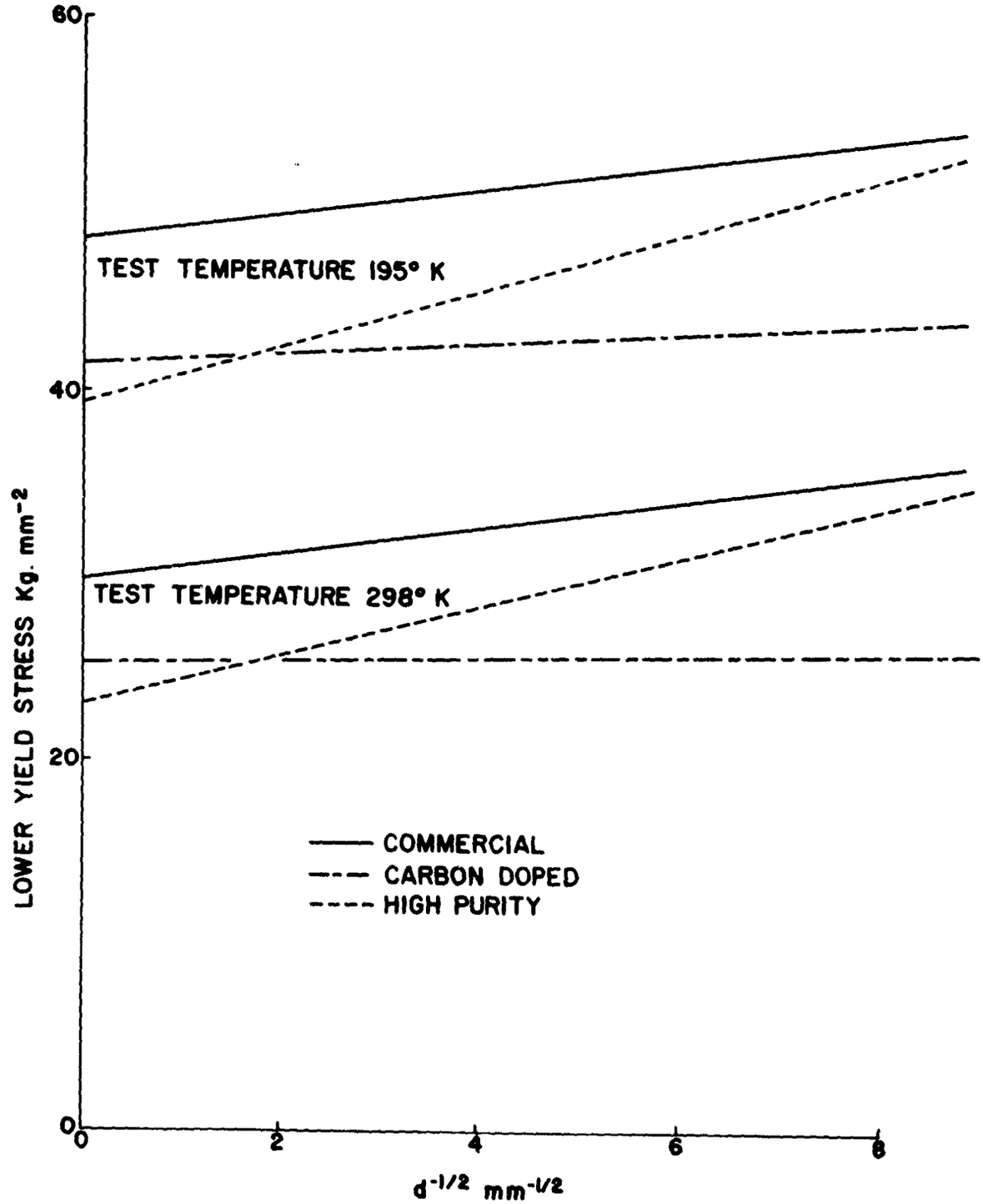

FIG. 16. COMPARATIVE LOWER YIELD STRESS/GRAIN SIZE PLOTS FOR A STRAIN RATE OF 10^{-1}/sec.

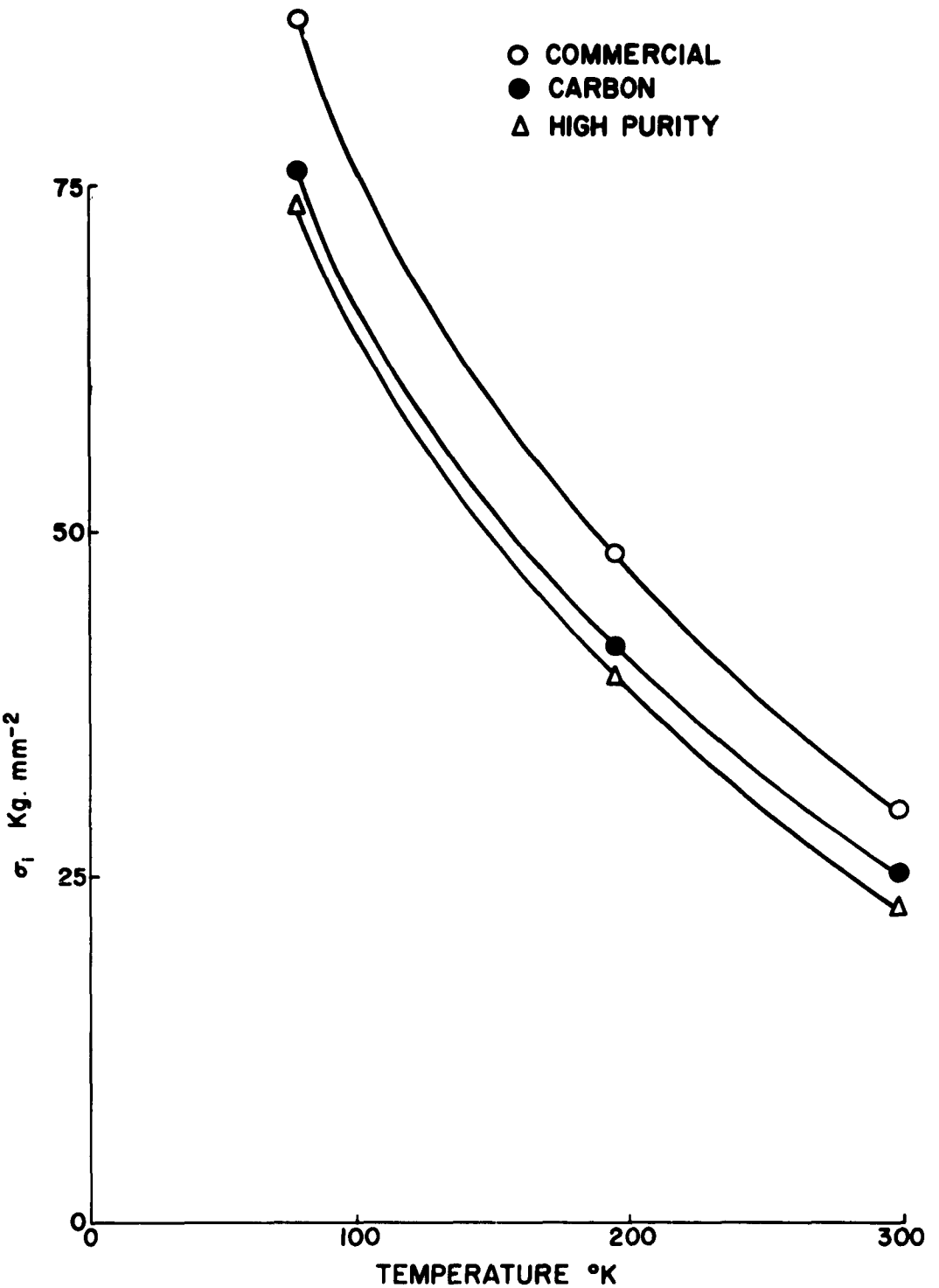

FIG. 17. COMPARATIVE σ_i TEMPERATURE BEHAVIOR FOR A STRAIN RATE OF 10^{-1}/sec.

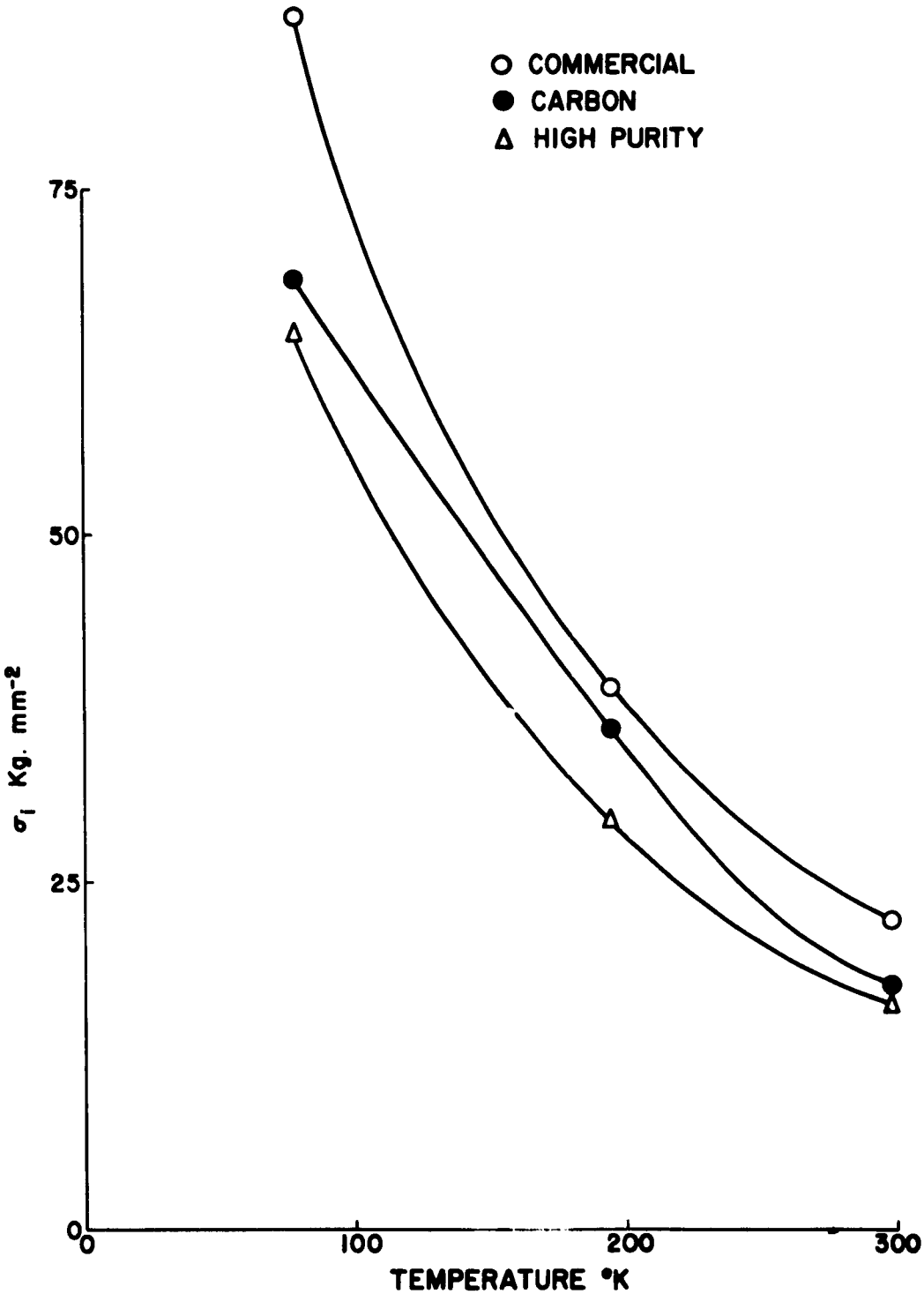

FIG. 18. COMPARATIVE σ_i TEMPERATURE BEHAVIOR FOR A STRAIN RATE OF 10^{-3}/sec.

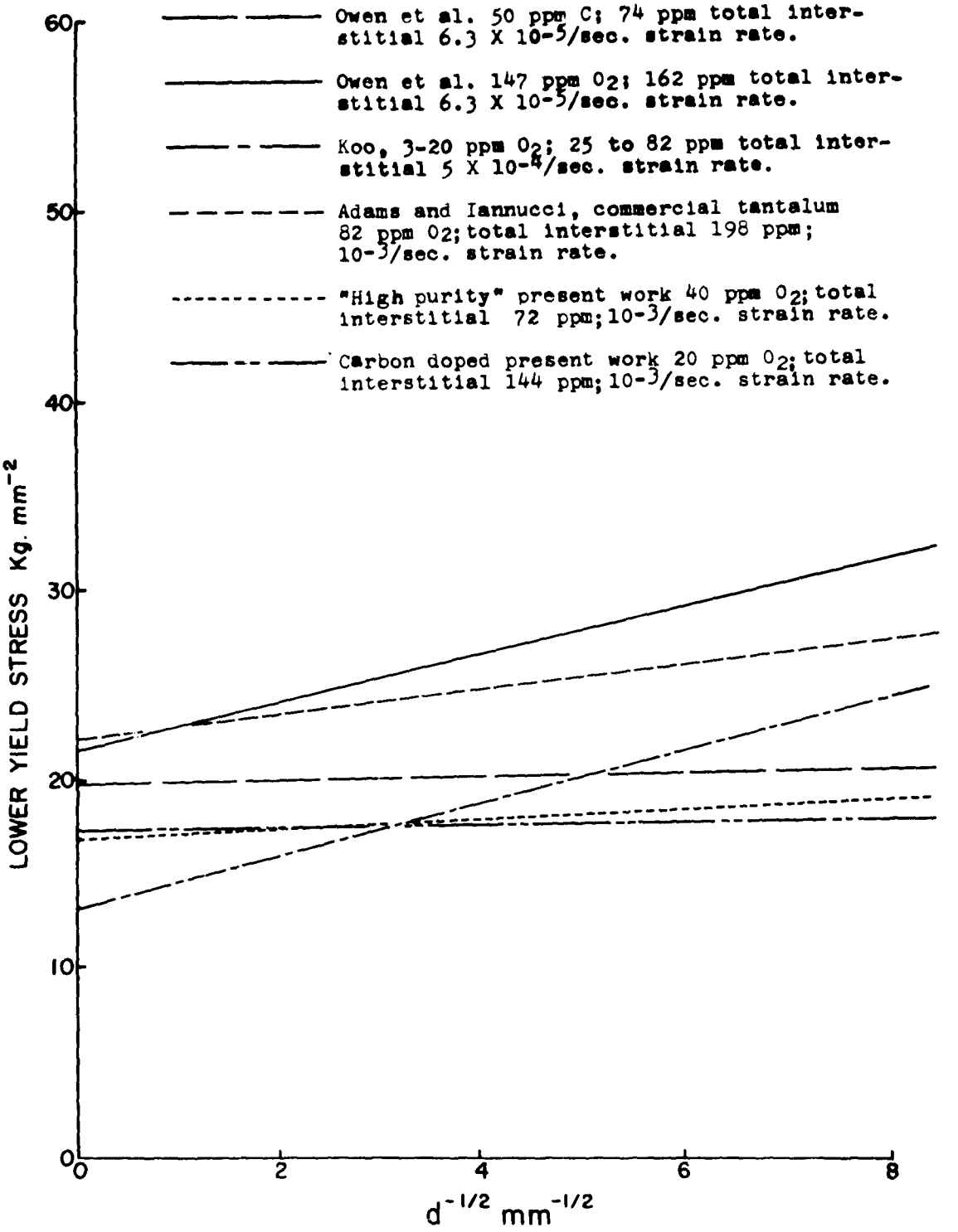

FIG. 19. COMPARISON OF YIELD STRENGTH-GRAIN SIZE RESULTS WITH THOSE OF OTHER INVESTIGATIONS. ROOM TEMPERATURE TESTS.

TABLE I

GRAIN SIZE vs APPROXIMATE RECRYSTALLIZATION TEMPERATURES

Temperature (°C)	Average Grain Size ($mm^{-1/2}$)	
	High Purity	Carbon Doped
1100	6.0	-
1200	3.8	-
1300	2.9	7.5
1400	1.9	6.0
1500	1.3	4.4
1600	0.9	3.5
1700	-	2.0

TABLE II

INTERSTITIAL CONTENT (PPM)

Material	Element O_2	C	N_2	H_2	Total (avg)
"High purity"	35,38,40	26,25,14	5,15,11	<1,<1,<1	72
Carbon doped	19,22,25	110,102,135	5,5,9	<1,<1,<1	~44
Commercial-Beam recrystallized, Adams and Iannucci	82	50	63	3	198
As-received	150	50	100	2	302

TABLE III

TENSILE AND FRACTURE PROPERTIES OF "HIGH PURITY" TANTALUM

Spec. No.	Temp. °K	Strain Rate Sec^{-1}	$d^{-1/2}$ mm$^{-1/2}$	L.Y.S.[1] Kg.mm^{-2}	U.Y.S.[2] Kg.mm^{-2}	U.T.S.[3] Kg.mm^{-2}	Uniform Elong. %	Elong. to Fracture %	Fracture Behavior[4]
B15c2			1.6	17.6	19.2	17.9	20.1	24.9	A
B21c2			2.8	16.8	16.8	17.9	11.0	17.4	B
B15b1			3.3	15.9	18.0	20.0	29.5	35.0	B
B18c1			3.6	18.0	18.8	21.4	15.9	20.6	B
B21a3		10^{-3}	3.6	17.9	18.5	23.0	-	-	A
B18b1			4.4	20.2	21.8	23.1	31.0	36.7	B
B19a1			4.6	18.6	19.9	23.4	27.5	33.8	B
B19a4			4.7	17.0	19.2	22.6	30.0	38.5	A
B19c1			5.2	17.6	18.4	23.4	24.9	31.0	A
B15a1	298		5.5	19.1	20.5	23.1	42.0	50.0	B
B20c1			1.6	25.5	29.1	-	20.0	26.4	B
B18a1			2.5	26.3	28.8	-	32.2	41.0	A
B16c3			3.5	27.0	27.0	-	27.1	35.1	B
B21a4			4.1	29.1	29.8	-	20.6	28.9	A
B18c2		10^{-1}	4.4	28.9	30.4	-	14.0	22.2	A
B19c2			4.7	28.3	30.0	29.0	27.8	35.0	A
B18b2			4.9	29.4	31.5	-	27.4	44.6	A
B19b1			4.9	29.5	29.8	-	15.5	27.0	A
B16a1			6.6	32.2	33.7	-	19.6	25.2	B

1. Lower Yield Stress
2. Upper Yield Stress
3. Ultimate Tensile Stress
4. A - Ragged Shear
   B.- Chisel Edge

TABLE III (Cont'd.)

Spec. No.	Temp. °K	Strain Rate Sec^{-1}	$d^{-1/2}$ mm$^{-1/2}$	L.Y.S.[1] Kg.mm^{-2}	U.Y.S.[2] Kg.mm^{-2}	U.T.S.[3] Kg.mm^{-2}	Uniform Elong. %	Elong. to Fracture %	Fracture[4] Behavior
B20c3			1.9	34.6	40.8	-	20.0	26.4	B
B21c2			1.9	33.8	35.0	-	14.8	22.6	B
B16c1			3.3	35.3	37.6	-	7.2	13.6	B
B16c4		10^{-3}	3.6	34.6	35.6	-	16.4	23.2	B
B21b1			3.6	35.5	39.4	-	13.0	19.4	A
B16b1			4.4	38.9	40.3	-	2.1	9.1	A
B19a2			4.4	37.8	38.7	-	15.3	21.7	A
B16a2	195		5.4	41.8	43.5	-	2.9	10.7	A
B21c3			2.1	44.5	46.5	-	8.5	13.8	B
B16c2			2.8	44.4	45.2	-	-	9.1	A
B21a1			3.5	42.5	45.3	-	-	12.7	A
B21b2		10^{-1}	3.5	44.8	46.4	-	5.0	12.5	B
B19a3			4.3	45.4	46.2	-	-	10.7	A
B17c2			4.7	46.6	50.7	-	7.6	12.5	B
B16b2			5.4	47.0	48.7	-	-	8.8	B
B16a3			6.0	51.1	54.6	-	-	9.3	A
B15c3	77		1.3	67.3	67.3	-	-	5.2	A
B15b3			3.2	68.5	68.5	-	-	6.2	B
B21b3			3.2	75.3	77.2	-	-	8.2	B
B15a3			3.6	71.0	71.0	-	-	6.6	B
B18b3		10^{-3}	3.8	74.3	78.2	-	-	7.0	A
B16b3			4.1	71.8	71.8	-	-	5.4	A
B17c3			4.4	75.1	75.1	-	-	7.4	B
B18c3			4.6	75.1	78.2	-	-	8.6	A

TABLE III (Cont'd.)

Spec. No.	Temp. °K	Strain Rate Sec^{-1}	$d^{-1/2}$ $mm^{-1/2}$	L.Y.S.[1] $Kg.mm^{-2}$	U.Y.S.[2] $Kg.mm^{-2}$	U.T.S.[3] $Kg.mm^{-2}$	Uniform Elong. %	Elong. to Fracture %	Fracture[4] Behavior
B20c2	77		1.6	78.8	81.8	-	-	7.4	B
B21a2			2.8	74.1	77.3	-	3.0	8.1	B
B19b4			3.2	76.3	76.3	-	-	5.6	A
B18a2		10^{-1}	3.5	77.2	80.9	-	3.9	9.8	A
B18b4			3.8	79.2	83.5	-	3.2	8.1	A
B18c4			4.3	78.5	80.6	-	2.6	8.3	A
B21b4			4.4	76.3	79.6	-	2.4	8.0	B
B16a4			5.5	82.7	84.8	-	1.2	7.0	A

TABLE IV

σ_i AND k_y VALUES BY PETCH METHOD
FOR HIGH PURITY TANTALUM

Temperature (°K)	Strain Rate (sec.)	σ_i $Kg.mm^{-2}$	k_y c.g.s. X 10^7
298	10^{-3}	16.2	0.66
298	10^{-1}	23.0	2.05
195	10^{-3}	29.6	3.03
195	10^{-1}	39.5	2.38
77	10^{-3}	64.8	3.39
77	10^{-1}	74.1	1.63

TABLE V

TENSILE AND FRACTURE PROPERTIES OF CARBON DOPED TANTALUM

Spec. No.	Temp. °K	Strain Rate Sec^{-1}	d$^{-1/2}$ mm$^{-1/2}$	L.Y.S.[1] Kg.mm^{-2}	U.Y.S.[2] Kg.mm^{-2}	U.T.S.[3] Kg.mm^{-2}	Uniform Elong. %	Elong. to Fracture %	Fracture[4] Behavior
B13b1	298	10^{-3}	1.6	17.6	18.9	20.8	14.1	17.3	B
B11a1			4.6	18.6	18.7	27.6	28.2	35.2	A
B11c1			4.7	18.1	18.8	25.7	30.2	37.5	A
B10d1			5.9	18.5	18.5	22.2	24.1	28.2	A
B12b1			7.3	18.5	18.5	28.0	23.0	31.2	A
B13c1		10^{-1}	2.2	24.2	24.7	24.3	15.3	22.0	B
B11c2			4.1	27.1	28.2	28.7	15	25.1	A
B10d2			4.7	26.4	27.9	28.4	24	32.9	A
B11a2			6.6	24.5	25.5	28.3	26.7	40.1	A
B12b2			6.6	25.7	26.4	28.4	20.6	32.4	A
B13b2	195	10^{-3}	1.6	33.3	33.3	34.4	14.6	20.7	B
B13a2			2.5	35.3	37.9	36.7	18.0	26.0	A
B11b2			4.6	34.6	36.0	35.8	17.0	26.2	A
B12a2			5.1	32.9	33.2	34.9	-	-	A
B10e2			7.6	32.5	33.8	35.7	18.7	29.6	A
B13c2		10^{-1}	1.9	40.5	43.9	-	3.5	9.0	B
B13a1			2.2	43.9	46.2	-	8.7	17.5	B
B11b3			4.3	44.0	45.4	-	6.5	13.2	A
B10e3			4.9	42.2	43.3	-	10.0	18.0	A

1. Lower Yield Stress
2. Upper Yield Stress
3. Ultimate Tensile Stress
4. A - Ragged Shear
   B - Chisel Edge

TABLE V (Cont'd.)

Spec. No.	Temp. °K	Strain Rate Sec^{-1}	$d^{-1/2}$ $mm^{-1/2}$	L.Y.S.[1] $Kg.mm^{-2}$	U.Y.S.[2] $Kg.mm^{-2}$	U.T.S.[3] $Kg.mm^{-2}$	Uniform Elong. %	Elong. to Fracture %	Fracture[4] Behavior
B13b3			1.6	64.1	67.5	-	-	4.5	B
B22a			2.4	71.2	73.1	-	2.2	6.3	A
B22b			2.8	71.2	71.2	-	-	-	A
B10e1			3.0	69.4	71.6	-	3.0	5.8	A
B13a3		10^{-3}	3.2	69.4	70.7	-	3.6	6.0	A
B22d			3.2	66.3	66.3	-	-	7.9	B
B22c			4.0	72.0	-	-	-	-	A
B11b1	77		4.1	69.6	71.4	-	3.4	7.8	A
B12a1			4.7	70.4	73.1	-	3.2	5.8	A
B13c3			2.2	77.7	81.4	-	-	7.0	A
B11c3			2.8	70.4	71.6	-	6.3	10.5	A
B10d3		10^{-1}	2.7	72.6	74.4	-	3.8	7.5	A
B11a3			5.7	69.3	70.8	69.4	9.7	14.2	A
B12a3			7.6	68.0	71.4	68.2	7.2	13.5	

TABLE VI

$\bar{\sigma}_i$ AND k_y VALUES BY PETCH METHOD FOR CARBON DOPED TANTALUM

Temperature (°K)	Strain Rate (sec.)	$\bar{\sigma}_i$ $Kg.mm^{-2}$	k_y $c.g.s. \times 10^7$
298	10^{-3}	17.5	0.24
298	10^{-1}	25.4	0.07
195	10^{-3}	36.0	0.83
195	10^{-1}	41.8	0.39
77	10^{-3}	68.7	0.22
77	10^{-1}	76.2	1.79

TABLE VII

RELATIVE STRAIN HARDENING COEFFICIENTS
FOR ROOM TEMPERATURE TESTS AT 10^{-1}/sec. STRAIN RATE

Material	Strain Hardening Coefficient
Carbon Doped	0.10
Commercial	0.095
"High Purity"	0.070

TABLE VIII

k_y - LUDERS STRAIN vs GRAIN SIZE METHOD
AT 298°K

Material	Spec. No.	Grain Size $d^{-1/2}$ ($mm^{-1/2}$)	Strain Rate $(sec)^{-1}$	k_y Luders Strain c.g.s. X 10^7	σ_i Luders Strain $Kg.mm^{-2}$	σ_i Grain Size Method $Kg.mm^{-2}$	k_y Grain Size Method c.g.s. X 10^7
"High Purity"	B20c1	1.6	10^{-1}	3.2	22.0	23.0	2.05
"	B19c2	4.7	10^{-1}	1.7	22.6		
"	B15c2	1.6	10^{-3}	4.1	13.8	16.2	0.66
"	B19a1	4.6	10^{-3}	1.0	16.9		
Carbon Doped	B13c1	2.2	10^{-1}	0.2	23.8	25.4	0.07
"	B10d2	4.7	10^{-1}	1.6	23.8		
"	B13b1	1.6	10^{-3}	1.8	13.3	17.5	0.25
"	B11c1	4.7	10^{-3}	0.4	17.1		

Aeronautical Systems Division, Dir/Materials and Processes. Metals and Ceramics Lab, Wright-Patterson AFB, Ohio
Rpt Nr ASD TR 61-203, Pt II. THE MECHANICAL PROPERTIES OF TANTALUM WITH SPECIAL REFERENCE TO THE DUCTILE-BRITTLE TRANSITION. Final report, Mar 63, 45p. incl illus., tables, and 14 refs.

Unclassified report

The lower yield stress-grain size relationship was studied in tantalum of two compositions; one consisting of a total interstitial content of 77 ppm with the major constituent being oxygen and the other containing carbon (116 ppm) in which part of the carbon was in the form of finely

(over)

dispersed carbide precipitate. The carbon containing material showed the lowest stresses. It was concluded that oxygen is much more effective than carbon in restricting dislocation movement. The effect of the carbide precipitate was to increase the work hardening rate. The flow stresses even in the presence of the carbide phase were lower than those observed for commercial tantalum.

k_y and σ_i values were computed.

1. Tantalum
2. Mechanical properties
3. Ductile-brittle transition
I. AFSC Project 7351, Task 735106
II. Contract AF 33 (616)-7173
III. Materials Research Corp., Orangeburg, New York
IV. G. T. Murray, R. A. Burn
V. Aval fr OTS
VI. In ASTIA collection

Aeronautical Systems Division, Dir/Materials and Processes. Metals and Ceramics Lab, Wright-Patterson AFB, Ohio
Rpt Nr ASD TR 61-203, Pt II. THE MECHANICAL PROPERTIES OF TANTALUM WITH SPECIAL REFERENCE TO THE DUCTILE-BRITTLE TRANSITION. Final report, Mar 63, 45p. incl illus., tables, and 14 refs.

Unclassified report

The lower yield stress-grain size relationship was studied in tantalum of two compositions; one consisting of a total interstitial content of 77 ppm with the major constituent being oxygen and the other containing carbon (116 ppm) in which part of the carbon was in the form of finely

(over)

dispersed carbide precipitate. The carbon containing material showed the lowest stresses. It was concluded that oxygen is much more effective than carbon in restricting dislocation movement. The effect of the carbide precipitate was to increase the work hardening rate. The flow stresses even in the presence of the carbide phase were lower than those observed for commercial tantalum.

k_y and σ_i values were computed.

1. Tantalum
2. Mechanical properties
3. Ductile-brittle transition
I. AFSC Project 7351, Task 735106
II. Contract AF 33 (616)-7173
III. Materials Research Corp., Orangeburg, New York
IV. G. T. Murray, R. A. Burn
V. Aval fr OTS
VI. In ASTIA collection